swollen in hypotonic buffer containing protease inhibitors followed by homogenization. Then, the post-nuclear supernatants were fractionated by ultracentrifugation on discontinuous sucrose gradients. All steps were carried out on ice. The fractions obtained were subjected to Western blotting with antibodies to Hck (clone 18; Transduction Laboratories), desmoglein (clone 62; Transduction Laboratories), annexin II (C-10; Santa Cruz), or calnexin (H-70; Santa Cruz).

Flow cytometry

Human myeloid TF-1-fms cells expressing Nef-ER fusion protein were maintained as described previously (Suzu et al., 2005; Hiyoshi et al., 2008). To activate the Nef-ER fusion protein, we used the estrogen analog 4-HT (Sigma) at a final concentration of 0.1 μM. The cells were stained with PE-labeled anti-Fms antibodies (Santa Cruz), and the level of cell surface Fms was analyzed by flow cytometry on a FACS Calibur using Cell Quest software (Becton Dickinson, Mountain View, CA).

Results

Analyses with Src kinase inhibitor and Hck mutant

As reported, Nef induces Fms maturation arrest when co-expressed with Hck in HEK293 cells (Fig. 1A). HEK293 cells do not express Hck endogenously, and the upper and lower band was the fully *N*-glycosylated and under-*N*-glycosylated Fms, respectively (Hiyoshi et al., 2008). The low molecular weight Fms was sensitive to Endo-H (Endo-β-*N*-acetylglucosaminindase H), which selectively cleaves high-mannose type oligosaccharide, and their increase was clearly associated with the intense staining of Fms mainly at

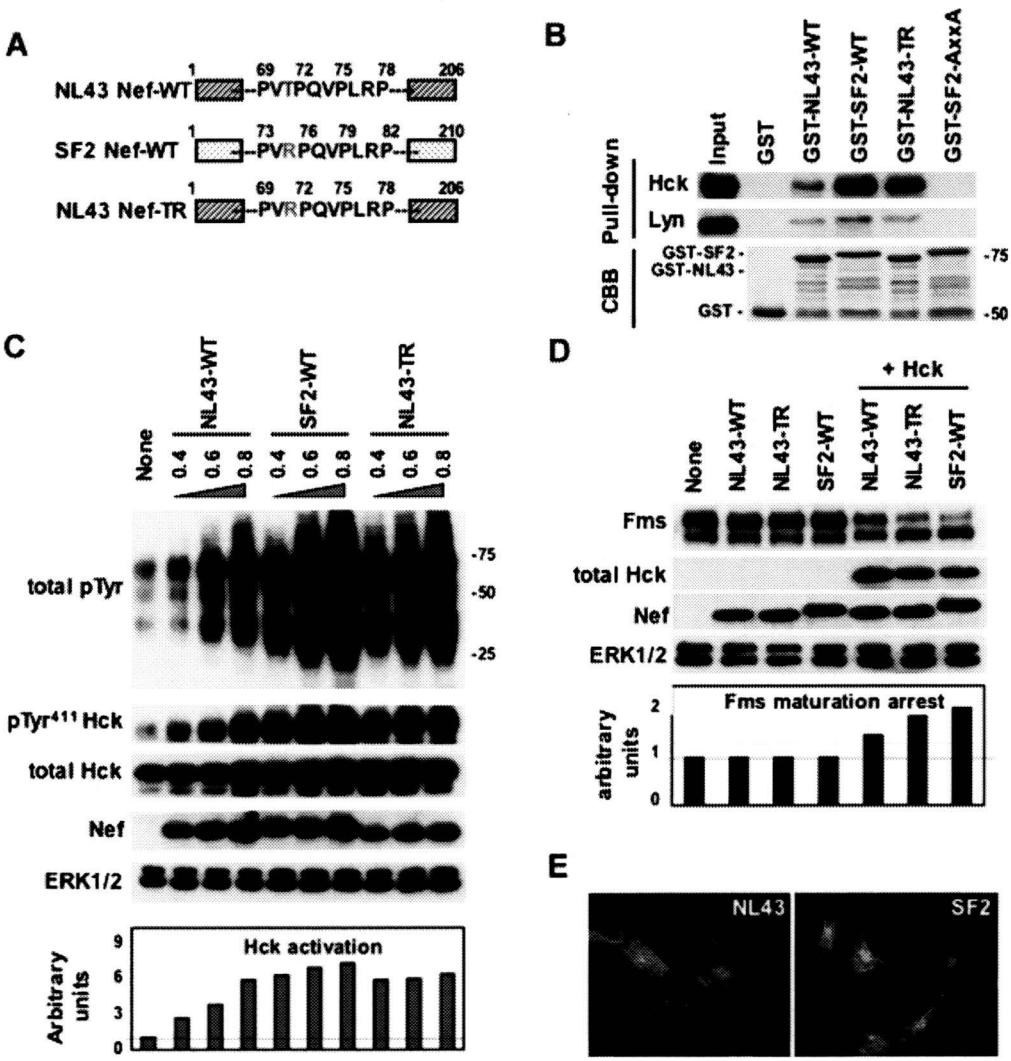

Fig. 3. Abilities of different Nef alleles to bind/activate Hck and to induce Fms maturation arrest. A: The NL43 Nef, SF2 Nef, and NL43 Nef-TR mutant used are schematically shown. B: The resins, to which the control GST or indicated GST-Nef proteins were bound, were incubated with the lysates of HEK293 cells expressing Hck or Lyn. The amount of Hck or Lyn bound to the resins was determined by Western blotting (Pull-down). The amount of GST and GST-Nef fusion proteins bound to the resins was verified by the elution from the resins followed by SDS–PAGE/Coomassie brilliant blue (CBB) staining. C: HEK293 cells were co-transfected with the wild-type Hck and indicated Nef alleles. The amounts of Nef plasmids used are shown (0.4, 0.6, or 0.8 μg/well). Total cell lysates were subjected to Western blotting with antibodies against phosphotyrosine (total pTyr), active-Hck (pTyr^{411}Hck), total Hck, CD8-Nef (Nef), or ERK by Western blotting. The quantified Hck activation is shown in the bar graph. D: Cells were transfected with Fms plasmid alone (None) or in combination with the plasmids for Nef and Hck, as indicated. Western blotting was done as in (C). E: Cells were transfected with indicated GFP-Nef plasmid (green). Nuclei were stained with DAPI (blue). [Color figure can be viewed in the online issue, which is available at www.interscience.wiley.com.]

the perinuclear region, which overlapped well with the signal of GM130 or Vti1a, the markers for the Golgi (Hiyoshi et al., 2008). These results strongly suggested that the low molecular weight Fms was the immature under-*N*-glycosylated form. The increase of the lower molecular weight species was obvious in the cells co-expressing Nef and Hck (Fig. 1A, left blot), and this Fms maturation arrest was blocked by a Src kinase inhibitor PP2 (Fig. 1A, right blot). However, the expression of a constitutive-active Hck mutant (Hck-P2A; Lerner and Smithgall, 2002) was not sufficient to induce Fms maturation arrest when expressed alone (Fig. 1B, Fms blot), despite its strong kinase activity (total pTyr and pTyr^{411} Hck blots). In this study, we monitored kinase activity of Hck by overall protein tyrosine-phosphorylation (total pTyr) and auto-phosphorylation of Hck (pTyr^{411} Hck) (reviewed in Korade-Mirnics and Corey, 2000). Nonetheless, Hck-P2A/Nef co-expression induced more severe Fms maturation arrest than wild-type Hck/Nef co-expression (Fig. 1B), and Nef did not enhance the kinase activity of Hck-P2A (Fig. 1C), confirming our previous finding that Hck activation was necessary but not sufficient for Nef-induced Fms maturation arrest.

Analyses with different Nef alleles and their mutants

In this study, we first found that Nef derived from SF2 strain of HIV-1 induced more severe Golgi-localization of Hck-P2A than Nef derived from NL43 strain. Hck-P2A signal at the plasma membrane was still observed in some NL43 Nef-transfected cells, whereas such signal was not observed in SF2 Nef-transfected cells (Fig. 2A). The Nef-induced skewed Golgi-localization of Hck-2PA was confirmed by a quantitative analysis, that is, subcellular fractionation on sucrose gradients. Based on a previous report (Matsuda et al., 2006), we used desmoglein, annexin II and calnexin as marker proteins for the plasma membrane, both the plasma membrane and the Golgi, and the endoplasmic reticulum, respectively. As shown (Fig. 2B), the plasma membrane was recovered in light fractions whereas the Golgi and the endoplasmic reticulum were recovered in heavy fractions, and the peak of Hck-P2A shifted to heavy fractions by the co-expression with NL43 Nef but not a Nef-AxxA mutant defective in the binding to Hck (Saksela et al., 1995). The peak shift was also associated with the appearance of many tyrosine-phosphorylated proteins in these fractions (Fig. 2B).

Both NL43 Nef and SF2 Nef had intact PxxP motif (Fig. 3A), but SF2 Nef showed much higher affinity to Hck than NL43 Nef (Fig. 3B). In the control experiments, we confirmed that the binding of both Nef to Lyn remained low and the PxxP motif-disrupted SF2 Nef mutant (AxxA) bound neither Hck nor Lyn. Reflecting the higher affinity to Hck, SF2 Nef induced stronger Hck activation (Fig. 3C) and more severe Fms maturation arrest (Fig. 3D). As expected, even SF2 Nef failed to induce Fms maturation arrest when co-expressed with Lyn (data not shown). However, SF2 Nef and NL43 Nef showed no obvious change in the pattern of predominant Golgi-localization (Fig. 3E). It was therefore likely that SF2 Nef bound Hck at

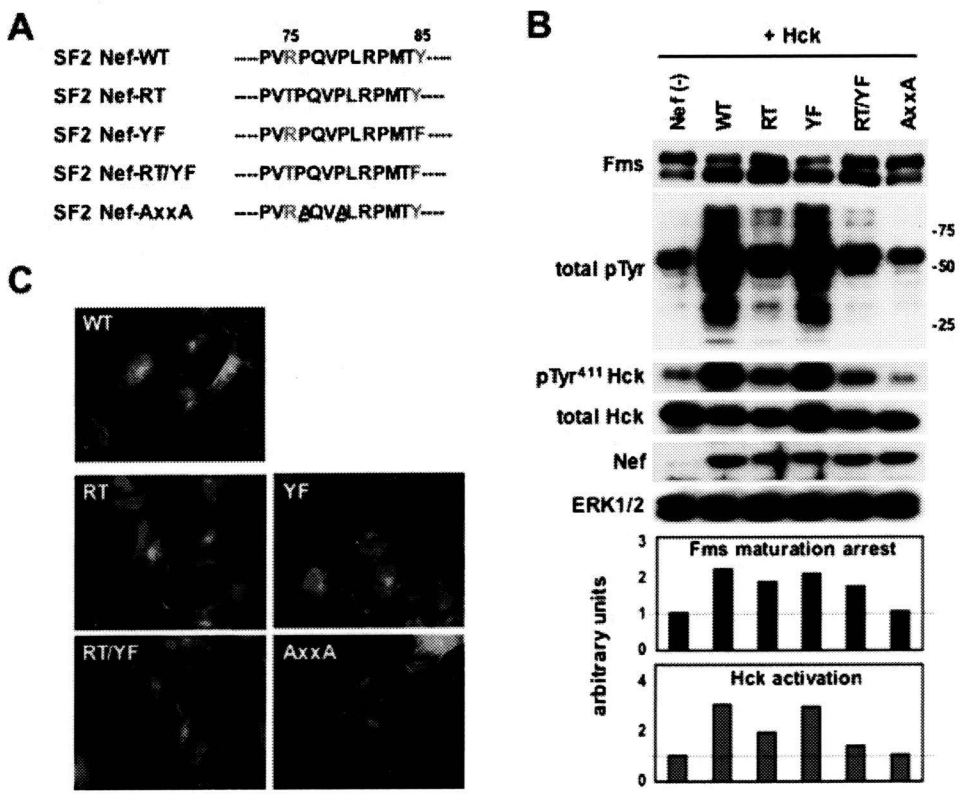

Fig. 4. Abilities of SF2 Nef mutants to activate Hck and to induce Fms maturation arrest. A: The SF2 Nef mutants used (RT, YF, RT/YF, and AxxA) are schematically shown. B: HEK293 cells were transfected with Fms plasmid alone (None) or in combination with the plasmids for Nef and Hck, as indicated. These cells were then analyzed for the expression of Fms, phosphotyrosine (total pTyr), active-Hck (pTyr^{411} Hck), total Hck, GFP-Nef (Nef), or ERK by Western blotting. The quantified Fms maturation arrest and Hck activation are shown in the bar graphs. C: Cells were transfected with indicated GFP-Nef plasmid (green). Nuclei were stained with DAPI (blue). [Color figure can be viewed in the online issue, which is available at www.interscience.wiley.com.]

the Golgi with higher affinity and thereby induced stronger Hck activation and more severe Fms maturation arrest.

There was a single amino acid difference within the PxxP motif, Thr^{71} in NL43 Nef and Arg^{75} in SF2 Nef (Fig. 3A). We found that an NL43 Nef with $Thr^{71}Arg$ substitution (NL43 Nef-TR) showed higher affinity to Hck than wild-type NL43 Nef (Fig. 3B), and induced stronger Hck activation (Fig. 3C) and more severe Fms maturation arrest (Fig. 3D) than wild-type NL43 Nef. We also performed a complementary experiment with SF2 Nef mutants (Fig. 4A; Ueno et al., 2008). As a result, we found that mutants with $Arg^{75}Thr$ substitution (SF2 Nef-RT and SF2-RT/YF) induced moderate Hck activation/Fms maturation arrest (Fig. 4B). However, both showed no obvious change in the pattern of predominant Golgi-localization (Fig. 4C). These results indicated that the single amino acid difference (Thr to Arg) within the PxxP motif governed the higher ability of SF2 Nef to induce Golgi-localization and activation of Hck, and Fms maturation arrest.

Although PxxP motif is essential for Nef to bind Hck, a recent study showed that an acidic region of Nef facilitated Nef-Hck binding at the Golgi (Hung et al., 2007). Although an NL43 Nef mutant lacking this region (ΔE; Fig. 5A) bound GST-Hck SH3 fusion proteins as with wild-type NL43 Nef (Fig. 5B), ΔE mutant was indeed less active than wild-type in transfected HEK293 cells, that is, in both Hck and activation Fms maturation arrest (Fig. 5C). Another mutant (M20; Fig. 5A), which was defective in the down-regulation of MHC I, another hallmark function of Nef (Akari et al., 2000), retained the ability to induce Hck activation and Fms maturation arrest (Fig. 5C). Both ΔE and M20A mutants showed no obvious change in the pattern of predominant Golgi-localization (Fig. 5C). The result further supported the idea that stronger Hck activation, which took place at the Golgi, induced severe Fms maturation arrest.

Analyses with a newly discovered Nef-Hck binding blocker

To directly show that the Golgi-localization of active Hck determines Nef-induced Fms maturation arrest, we sought to discover Nef-Hck binding blockers. In this study, we focused on UCS15A and its analogs 2b and 2c (Fig. 6A), because these small-molecule compounds were shown to block several proline-rich motif-SH3 domain binding such as Sam68-Fyn binding (Oneyama et al., 2003) and AMAP1-cortactin binding (Hashimoto et al., 2006). As they have not been used before for HIV-1 studies, we tested their capability to block Nef-Hck binding by the GST pull-down assay. As shown (Fig. 6B), all compounds blocked the binding of Hck to NL43 Nef or NL43 Nef-TR mutant (more potent than the wild-type, see Fig. 3), in a dose-dependent manner. Like the case of Sam68-Fyn binding (Oneyama et al., 2003), 2c was the most effective in blocking Nef-Hck binding (Fig. 6B), and showed no obvious toxicity to HEK293 cells (Fig. 6C). As shown (Fig. 6D), 2c indeed inhibited

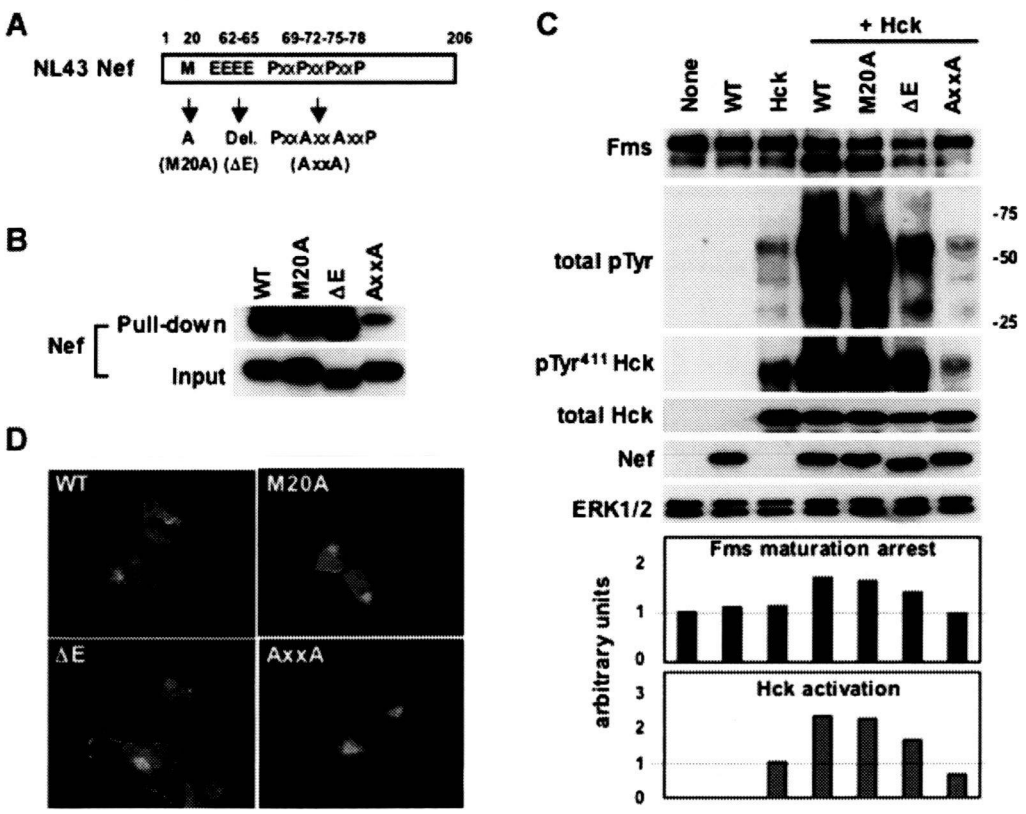

Fig. 5. Abilities of NL43 Nef mutants to activate Hck and to induce Fms maturation arrest. A: The NL43 Nef mutants used (M20A, ΔE, and AxxA) are schematically shown. B: The resin, to which GST-Hck SH3 fusion proteins were bound, were incubated with the lysates of HEK293 cells expressing the indicated Nef proteins. The amount of Nef proteins in the lysates (Input) or bound to the resins (Pull-down) was verified by Western blotting. C: HEK293 cells were transfected with Fms plasmid alone (None) or in combination with the plasmids for Nef and Hck, as indicated. These cells were then analyzed for the expression of Fms, phosphotyrosine (total pTyr), active-Hck ($pTyr^{411}$ Hck), total Hck, CD8-Nef (Nef), or ERK by Western blotting. The quantified Fms maturation arrest and Hck activation are shown in the bar graphs. D: Cells were transfected with indicated GFP-Nef (green). Nuclei were stained with DAPI (blue). [Color figure can be viewed in the online issue, which is available at www.interscience.wiley.com.]

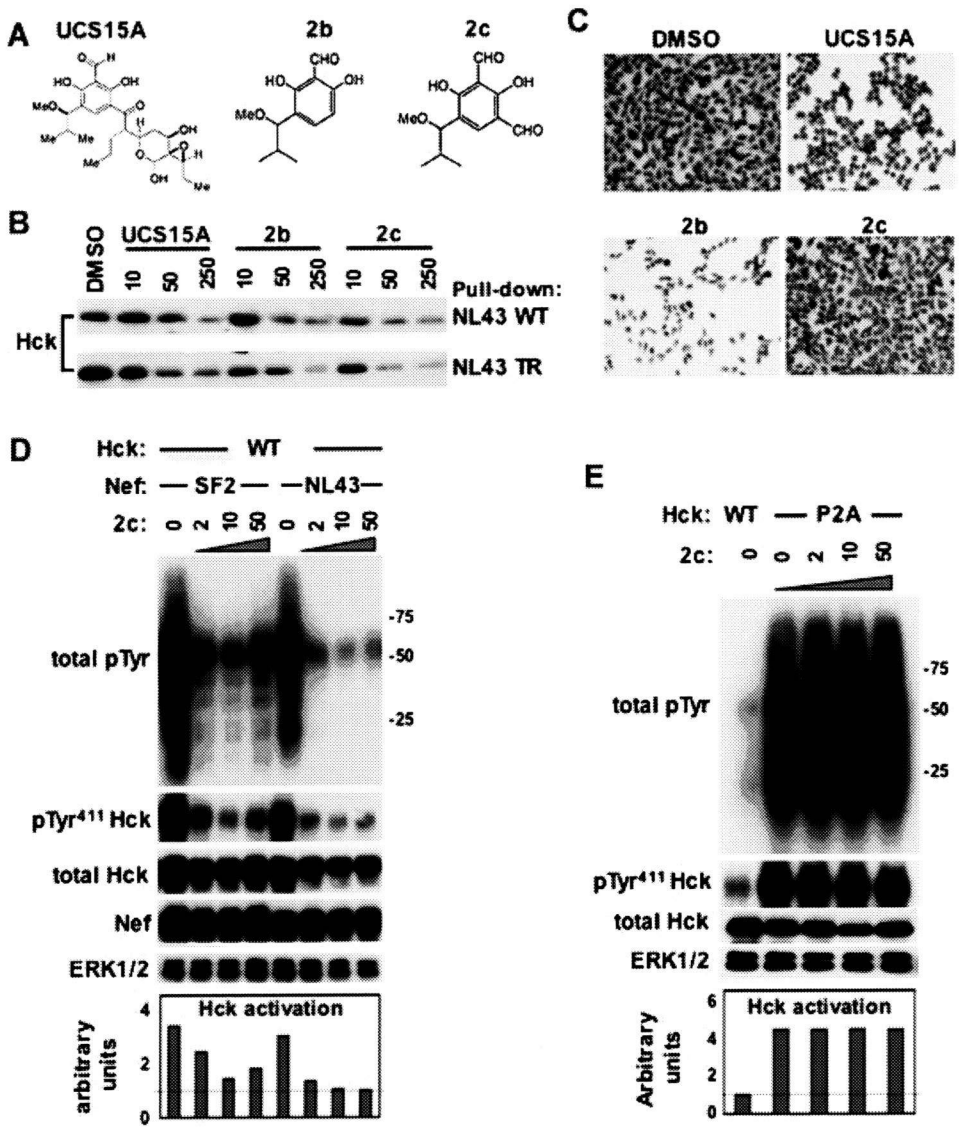

Fig. 6. Capability of 2c to block Nef-Hck binding and Nef-induced Hck activation. A: Chemical structures of UCS15A, 2b, and 2c are shown. B: The resins, to which GST-Nef (NL43 wild-type or TR mutant, see Fig. 2A) proteins were bound, were incubated with the lysates of Hck-expressing HEK293 cells in the absence (DMSO) or presence of the indicated concentration (0, 10, 50, or 250 μM) of UCS15A, 2b, or 2c. The amount of Hck proteins bound to the resins was determined by Western blotting. C: HEK293 cells were cultured in the absence (DMSO) or presence of 50 μM of UCS15A, 2b, or 2c for 2 days, and subjected to Wright-Giemsa staining. D: Cells were co-transfected with Hck-WT and indicated Nef alleles (SF2 or NL43), and cultured in the presence of increasing concentrations (μM) of 2c. These cells were then analyzed for the expression of tyrosine-phosphorylated proteins (total pTyr), active-Hck (pTyr^{411}Hck), total Hck, CD8-Nef (Nef), or ERK by Western blotting. The quantified Hck activation is shown in the bar graphs. E: Cells were transfected with Hck-WT or Hck-P2A, and cultured in the presence of increasing concentrations (μM) of 2c. These cells were analyzed as in (D). [Color figure can be viewed in the online issue, which is available at www.interscience.wiley.com.]

Hck activation by NL43 Nef and more potent SF2 Nef (see Fig. 3). Importantly, 2c had little inhibitory effect on kinase activity of the constitutive-active Hck P2A mutant, even when used at a concentration as high as 50 μM (Fig. 6E). These results indicated that 2c was not a kinase inhibitor but inhibited Nef-induced Hck activation by blocking Nef-Hck binding.

This unique feature of 2c prompted us to examine whether 2c blocks Nef/Hck-induced Fms maturation arrest and Nef-induced skewed Golgi-localization of Hck. As shown (Fig. 7A), 2c completely blocked Fms maturation arrest induced by Nef and wild-type Hck as expected. However, of particular importance was that 2c also completely blocked severe Fms maturation arrest induced by Nef and the constitutive-active Hck P2A (Fig. 7B). Because 2c had little inhibitory effect on kinase activity of Hck-P2A (see Fig. 6E), these results strongly supported that the presence of Hck-P2A at the Golgi caused by its binding with Nef (see Fig. 2) was a direct cause of severe Fms maturation arrest. We therefore sought to verify that 2c indeed blocked Nef-induced skewed Golgi-localization of Hck-P2A. To this end, we employed the quantitative analysis, that is, subcellular fractionation on sucrose gradients (see Fig. 2B). The peak of Hck-P2A shifted to heavier fractions by the co-expression with Nef, and such change in the intracellular localization of Hck-P2A was restored to normal by the addition of 2c (Fig. 7C). We also tested whether 2c blocked Nef-induced Fms abnormality in another culture system. We previously showed that the cell surface expression of Fms was impaired in human myeloid TF-1-fms cells expressing a conditionally active

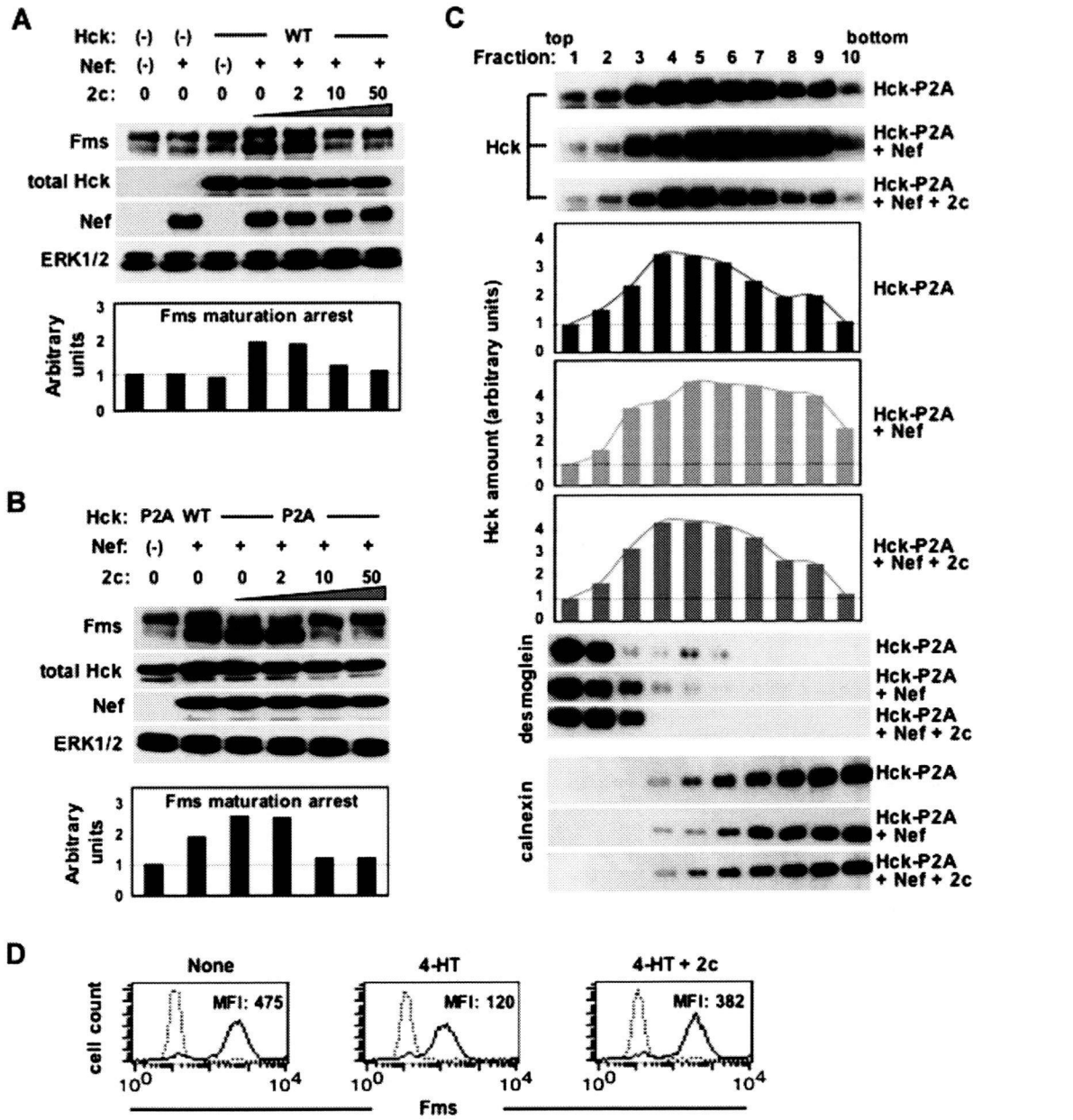

Fig. 7. Capability of 2c to block Fms maturation arrest and skewed Golgi-localization of Hck. A: HEK293 cells were transfected with the plasmids (Fms, NL43 Nef, and Hck-WT) in combination indicated, and cultured in the presence of increasing concentrations (μM) of 2c. These cells were then analyzed for the expression of Fms, total Hck, CD8-Nef (Nef), or ERK by Western blotting. The quantified Fms maturation arrest is shown in the bar graphs. B: Cells were transfected with the plasmids (Fms, NL43 Nef, Hck-WT, and Hck-P2A) in combination indicated, and cultured in the presence of increasing concentrations (μM) of 2c. These cells were then analyzed as in A. C: Cells were transfected with Hck-P2A alone (top), or co-transfected with NL43 Nef (middle). 2c was added to a final concentration of 50 μM to selected wells (bottom). Then, cells were subjected to subcellular fractionation on sucrose gradients and Hck Western blotting. The quantified Hck amounts are shown in the bar graph. The fractions were also analyzed for the amount of desmoglein and calnexin. D: TF-1-fms-Nef-ER cells cultured with M-CSF-free media in the absence (left) or presence of 0.1 μM 4-HT (middle), or the co-presence of 0.1 μM 4-HT and 50 μM 2c (right) for 12 h. The expression of Fms on the surface of treated cells was analyzed by flow cytometry with PE-labeled anti-Fms. The mean fluorescence intensity (MFI) of Fms expression is indicated. [Color figure can be viewed in the online issue, which is available at www.interscience.wiley.com.]

Nef-ER fusion protein when the Nef-ER in the cells was activated by the estrogen analog 4-HT (Hiyoshi et al., 2008). This impaired cell surface Fms expression was highly likely due to intracellular Fms maturation arrest (Hiyoshi et al., 2008). Finally, we found that the Fms down-regulation in Nef-active TF-1-fms-Nef-ER cells was also restored to normal by the addition of 2c (Fig. 7D). All taken together, our present study clearly demonstrated that skewed Golgi-localization of active Hck induced by Nef was indeed the direct cause of Fms maturation arrest.

Discussion

M-CSF is a cytokine essential not only for the survival of macrophages but also for the maintenance of macrophages at an

anti-inflammatory state (reviewed in Chitu and Stanley, 2006; Hamilton, 2008). Thus, the inhibitory effect of Nef on M-CSF signal through Fms maturation arrest at the Golgi is a possible trigger to worsen uncontrolled immune systems in patients (Suzu et al., 2005; Hiyoshi et al., 2008). In this study, we therefore sought to define molecular basis of this important function of Nef, by using different Nef alleles, various Nef mutants, constitutive-active Hck mutant, and Nef-Hck binding blocker 2c. The study with various Nef proteins supported the idea that high affinity Nef-Hck binding and subsequent stronger Hck activation, both of which took place mainly at the Golgi, determined Fms maturation arrest at the Golgi (Figs. 2–5). Moreover, the study with 2c enabled us to conclude that skewed Golgi-localization of active Hck by Nef was indeed the direct cause of Fms maturation arrest (Figs. 6 and 7). By analogy with the Sam68-Fyn binding inhibition (Oneyama et al., 2003), the inhibitory effect of 2c on Nef-Hck binding was supposed to be mediated by its interaction with Nef PxxP motif.

As mentioned earlier, it has been known for a long time that most members of Src kinases including Hck localize to the Golgi as well as to the plasma membrane. For example, it was shown that newly synthesized Lyn initially localized and accumulated to the Golgi, and then moved toward the plasma membrane (Kasahara et al., 2004). Importantly, Pulvirenti et al. (2008) recently revealed that coordinated regulation of activity of the Golgi-localized Src kinases is crucial to maintain intra-Golgi trafficking of proteins. Our present finding that skewed Golgi-localization of active Hck leads to Fms maturation arrest at the Golgi is in line with the new concept. It appears that long-lasting and dys-regulated activation of the Golgi-localized Src kinases disturbs glycosylation and/or trafficking of proteins, exemplified by Fms maturation arrest. Indeed, N-Src, a c-Src isoform with a higher basal tyrosine kinase activity (Brugge et al., 1985), showed more obvious perinuclear localization than the constitutive-active Hck-P2A and induced Fms maturation arrest even in the absence of Nef (unpublished result). Moreover, Mitina et al. (2007) reported that over-expression of an active form of Hck disturbed *N*-glycosylation of another cytokine receptor Flt3 even in the absence of Nef. These results may further support the idea that long-lasting and dys-regulated activation of the Golgi-localized Src kinases per se affects protein glycosylation and/or trafficking at the Golgi. Anyhow, our system with Nef provides a useful model to elucidate how Src kinases regulate the Golgi structure/function. It will be important to identify which Golgi proteins are phosphorylated directly or indirectly by Hck activated at the Golgi and to clarify how such phosphorylation cascade leads to Nef-induced Fms maturation arrest.

Nef has been shown to affect protein trafficking and a well-characterized target is major histocompatibility complex class I (MHC I). Nef reduced the cell surface expression of MHC I, which diminishes the recognition of infected cells by cytotoxic T cells (reviewed in Fackler and Baur, 2002; Peterlin and Trono, 2003). However, it is still in intense debate whether Nef requires SH3 domain-containing proteins such as Hck to reduce the cell surface level of MHC I (Schwartz et al., 1996; Greenberg et al., 1998; Mangasarian et al., 1999; Akari et al., 2000; Chang et al., 2001; Roeth and Collins, 2006; Hung et al., 2007; Atkins et al., 2008). In this regard, Fms is not the direct target of Nef. However, as shown, Nef disturbed the cell surface expression of Fms, which is triggered by skewed Golgi-localization of active Hck. Moreover, it was shown that Nef disturbed the cell surface expression of another macrophage-specific protein HFE, an iron homeostasis regulator, which was blocked by a dominant-negative Hck (Drakesmith et al., 2005). Although whether the reduced cell surface level of HFE by Nef relates to skewed Golgi-localization of active Hck is unclear, it is conceivable that Nef acquires an additional machinery to manipulate protein trafficking in macrophages by exploiting the Golgi-localized Hck. Of interest, the *N*-glycosylation of Flt3, which is structurally related to Fms, was also impaired in Nef/Hck-expressing HEK293 cells, but the degree of maturation arrest of Flt3 was quite weak when compared to that of Fms (data not shown). The finding may imply that Fms maturation arrest is not necessarily due to the general disruption in the Golgi structure or function. Future studies, in which we determine to what extent overall protein *N*-glycosylation and trafficking are affected by Nef-Hck binding, will further clarify pathological significance of the molecular binding in macrophages. The newly discovered Nef-Hck binding blocker 2c will be useful in such studies and may provide a strategy to complement current anti-HIV-1 therapy for better treatment outcomes.

In this study, we showed that SF2 Nef had much higher affinity to Hck than NL43 Nef and thereby induced stronger Hck activation/severe Golgi-localization of Hck (Figs. 2 and 3) and that the single amino acid difference (Thr^{71} in NL43 Nef and Arg^{75} in SF2 Nef) within PxxP motif largely governs the higher ability of SF2 Nef (Figs. 3 and 4). This difference might reflect that the $Thr^{71}Arg$ substitution in NL43 Nef (NL43 Nef-TR, see Fig. 3) altered the flexibility of a loop containing the PxxP motif (Fackler et al., 2001). Importantly, for reasons not clearly understood, NL43 Nef-TR was more pathogenic in HIV-1 Tg mice than wild-type NL43 Nef and the pathogenicity of SF2 Nef in Tg mice was evident despite very low levels of expression (Priceputu et al., 2007). It is therefore possible that more severe Golgi-localization of active Hck followed by perturbed *N*-glycosylation and trafficking of proteins including Fms account for the high pathogenicity of SF2 Nef in Tg mice.

In summary, our present study clearly demonstrated that skewed Golgi-localization of active Hck was the direct cause of Fms maturation arrest by Nef. Our findings establishes an intriguing link between the pathogenesis of HIV-1 Nef and the newly emerging concept that the Golgi-localized Src kinases regulate the Golgi function. The identification of Golgi proteins phosphorylated by the Golgi-localized active Hck will provide novel insights into molecular mechanisms by which Nef functions as an HIV-1 pathogenetic factor through Hck and the Gogi-localized Src kinases regulate the Golgi function.

Acknowledgments

We thank Dr. G. Thomas (Vollum Institute) for critical reading of the manuscript. We thank Ms. Y. Endo and Ms. I. Suzu for experimental assistance.

Literature Cited

Akari H, Arold S, Fukumori T, Okazaki T, Strebel K, Adachi A. 2000. Nef-induced major histocompatibility complex class I down-regulation is functionally dissociated from its virion incorporation, enhancement of viral infectivity, and CD4 down-regulation. J Virol 74:2907–2912.

Arold S, O'Brien R, Franken P, Strub MP, Hoh F, Dumas C, Ladbury JE. 1998. RT loop flexibility enhances the specificity of Src family SH3 domains for HIV-1 Nef. Biochemistry 37:14683–14691.

Atkins KM, Thomas L, Youker RT, Harriff MJ, Pissani F, You H, Thomas G. 2008. HIV-1 Nef binds PACS-2 to assemble a multikinase cascade that triggers major histocompatibility complex class I (MHC-I) down-regulation: Analysis using short interfering RNA and knockout mice. J Biol Chem 283:11772–11784.

Bard F, Mazelin L, Pechoux-Longin C, Malhotra V, Jurdic P. 2003. Src regulates Golgi structure and KDEL receptor-dependent retrograde transport to the endoplasmic reticulum. J Biol Chem 278:46601–46606.

Bijlmakers MJ, Isobe-Nakamura M, Ruddock LJ, Marsh M. 1997. Intrinsic signals in the unique domain target p56lck to the plasma membrane independently of CD4. J Cell Biol 137:1029–1040.

Brugge JS, Cotton PC, Queral AE, Barrett JN, Nonner D, Keane RW. 1985. Neurones express high lenels of a structurally modified, activated form of pp60c-src. Nature 316:554–557.

Carreno S, Gouze ME, Schaak S, Emorine LJ, Maridonneau-Parini I. 2000. Lack of palmitoylation redirects $p59^{Hck}$ from the plasma membrane to $p61^{Hck}$-positive lysosomes. J Biol Chem 275:36223–36229.

Chang AH, O'Shaughnessy MV, Jirik FR. 2001. Hck SH3 domain-dependent abrogation of Nef-induced class I MHC down-regulation. Eur J Immunol 31:2382–2387.

Chitu V, Stanley ER. 2006. Colony-stimulating factor-1 in immunity and inflammation. Curr Opin Immunol 18:39–48.

David-Pfeuty T, Nouvian-Dooghe Y. 1990. Immunolocalization of the cellular src protein in interphase and mitotic NIH c-src overexpresser cells. J Cell Biol 111:3097–3116.
Deacon NJ, Tsykin A, Solomon A, Smith K, Ludford-Menting M, Hooker DJ, McPhee DA, Greenway AL, Ellett A, Chatfield C, Lawson VA, Crowe S, Maerz A, Sonza S, Learmont, Sullivan JS, Cunningham A, Dwyer D, Mills J. 1995. Genomic structure of an attenuated quasi species of HIV-1 from a blood transfusion and recipients. Science 270:988–991.
Drakesmith H, Chen N, Ledermann H, Screaton G, Townsend A, Xu XN. 2005. HIV-1 Nef down-regulates the hemochromatosis protein HFE, manipulating cellular iron homeostasis. Proc Natl Acad Sci USA 102:11017–11022.
Fackler OT, Baur AS. 2002. Live and let die: Nef functions beyond HIV replication. Immunity 16:493–497.
Fackler OT, Wolf D, Weber HO, Laffert B, D'Aloja P, Schuler-Thurner B, Geffin R, Saksela K, Geyer M, Peterlin BM, Schuler G, Baur AS. 2001. A natural variability in the proline-rich motif of Nef modulates HIV-1 replication in primary T cells. Curr Biol 11:1294–1299.
Greenberg ME, Iafrate AJ, Skowronski J. 1998. The SH3 domain-binding surface and an acidic motif in HIV-1 nef regulate trafficking of class I MHC complexes. EMBO J 17:2777–2789.
Haller C, Rauch S, Fackler OT. 2007. HIV-1 Nef employs two distinct mechanisms to modulate Lck subcellular localization and TCR induced actin remodeling. PLoS ONE 2:e1212.
Hamilton JA. 2008. Colony-stimulating factors in inflammation and autoimmunity. Nat Rev Immunol 8:533–544.
Hanna Z, Kay DG, Rebai N, Guimond A, Jothy S, Jolicoeur P. 1998. Nef harbors a major determinant of pathogenicity for and AIDS-like disease induced by HIV-1 in transgenic mice. Cell 95:163–175.
Hanna Z, Weng X, Kay DG, Poudrier J, Lowell C, Jolicoeur P. 2001. The pathogenicity of human immunodeficiency virus (HIV) type 1 Nef in CD4C/HIV transgenic mice is fabolished by mutation of its SH3-binding domain, and disease development is delayed in the absence of Hck. J Virol 75:9378–9392.
Hashimoto S, Hirose M, Hashimoto A, Morishige M, Yamada A, Hosaka H, Akagi K, Ogawa E, Oneyama C, Agatsuma T, Okada M, Kobayashi H, Wada H, Nakano H, Ikegami T, Nakagawa A, Sabe H. 2006. Targeting AMAP1 and cortactin binding bearing an atypical src homology 3/proline interface for prevention of breast cancer invasion and metastasis. Proc Natl Acad Sci USA 103:7036–7041.
Hiyoshi M, Suzu S, Yoshidomi Y, Hassan R, Harada H, Sakashita N, Akari H, Motoyoshi K, Okada S. 2008. Interaction between Hck and HIV-1 Nef negatively regulates cell surface expression of M-CSF receptor. Blood 111:243–250.
Hung CH, Thomas L, Ruby CE, Atkins KM, Morris NP, Knight ZA, Scholz I, Barklis E, Weinberg AD, Shokat KM, Thomas G. 2007. HIV-1 Nef assembles a Src family kinase-ZAP-70/Syk-PI3K cascade to down-regulate cell surface MHC-I. Cell Host Microbe 1:121–133.
Kaplan KB, Swedlow JR, Varmus HE, Morgan DO. 1992. Association of $p60^{c\text{-}src}$ with endosomal membranes in mammalian fibroblasts. J Cell Biol 118:321–333.
Karkkainen S, Hiipakka M, Wang JH, Kleino I, Vaha-Jaakkola M, Renkema GH, Kiss M, Wagner R, Saksela K. 2006. Identification of preferred protein interactions by phage-display of the human Src homology-3 proteome. EMBO Rep 7:186–191.
Kasahara K, Nakayama Y, Ikeda K, Fukushima Y, Matsuda D, Horimoto S, Yamaguchi N. 2004. Trafficking of Lyn through the Golgi caveolin involves the charged residues on αE and αI helices in the kinase domain. J Cell Biol 165:641–652.
Kestler HW III, Ringler DJ, Mori K, Panicali DL, Sehgal PK, Daniel MD, Desrosiers RC. 1991. Importance of the nef gene for maintenance of high virus loads and for development of AIDS. Cell 65:651–662.
Kirchhoff F, Greenough TC, Brettler DB, Sullivan JL, Desrosiers RC. 1995. Brief report: Absence of intact nef sequences in a long-term survivor with nonprogressive HIV-1 infection. N Engl J Med 332:228–232.
Korade-Mirnics Z, Corey SJ. 2000. Src kinase-mediated signaling in leukocytes. J Leukocyte Biol 68:603–613.
Lerner EC, Smithgall TE. 2002. SH3-dependent stimulation of Src-family kinase autophosphorylation without tail release from the SH2 domain in vivo. Nat Struct Biol 9:365–369.
Ley SC, Marsh M, Bebbington CR, Proudfoot K, Jordan P. 1994. Distinct intracellular localization of Lck and Fyn protein tyrosine kinases in human T lymphocytes. J Cell Biol 125:639–649.
Lowell CA. 2004. Src-family kinases: Rheostats of immune cell signaling. Mol Immunol 41:631–643.
Mangasarian A, Piguet V, Wang JK, Chen YL, Trono D. 1999. Nef-induced CD4 and major histocompatibility complex class I (MHC-I) down-regulation are governed by distinct determinants: N-terminal alpha helix and proline repeat of Nef selectively regulate MHC-I trafficking. J Virol 73:1964–1973.
Matsuda D, Nakayama Y, Horimoto S, Kuga T, Ikeda K, Kasahara K, Yamaguchi N. 2006. Involvement of Golgi-associated Lyn tyrosine kinase in the translocation of annexin II to the endoplasmic reticulum under oxidative stress. Exp Cell Res 312:1205–1217.
Mitina O, Warmuth M, Krause G, Hallek M, Obermeier A. 2007. Src family tyrosine kinases phosphorylate Flt3 on juxtamembrane tyrosines and interfere with receptor maturation in a kinase-dependent manner. Ann Hematol 86:777–785.
Moarefi I, LaFevre-Bernt M, Sicheri F, Huse M, Lee CH, Kuriyan J, Miller WT. 1997. Activation of the Src-family tyrosine kianse Hck by SH3 domain displacement. Nature 385:650–653.
Oneyama C, Agatsuma T, Kanda Y, Nakano H, Sharma SV, Nakano S, Narazaki F, Tatsuta K. 2003. Synthetic inhibitors of proline-rich ligand-mediated protein-protein interaction: Potent analogs of UCS15A. Chem Biol 10:443–451.
Paliwal P, Radha V, Swarup G. 2007. Regulation of p73 by Hck through kinase-dependent and independent mechanisms. BMC Mol Biol 8:45.
Peterlin BM, Trono D. 2003. Hide, shield and strike back: How HIV-infected cells avoid immune eradication. Nat Rev Immunol 3:97–107.
Priceputu E, Hanna Z, Hu C, Simard MC, Vincent P, Wildum S, Schindler M, Kirchhoff F, Jolicoeur P. 2007. Primary human immunodeficiency virus type 1 Nef alleles show major differences in pathogenicity in transgenic mice. J Virol 81:4677–4693.
Pulvirenti T, Giannotta M, Capestrano M, Capitani M, Pisanu A, Polishchuk RS, San Pietro E, Beznoussenko GV, Mironov AA, Turacchio G, Hsu VW, Sallese M, Luini A. 2008. A traffic-activated Golgi-based signaling circuit coordinates the secretory pathway. Nat Cell Biol 10:912–922.
Roeth JF, Collins KL. 2006. Human immunodeficiency virus type 1 Nef: Adapting to intracellular trafficking pathways. Mol Biol Rev 70:548–563.
Saksela K, Cheng G, Baltimore D. 1995. Proline-rich (PxxP) motifs in HIV-1 Nef bind to SH3 domains of a subset of Src kinases and are required for the enhanced growth of Nef^{+} viruses but not for down-regulation of CD4. EMBO J 14:484–491.
Schwartz O, Marechal V, Le Gall S, Lemonnier F, Heard JM. 1996. Endocytosis of major histocompatibility complex class I molecules is induced by the HIV-1 Nef protein. Nat Med 2:338–342.
Suzu S, Tanaka-Douzono M, Nomaguchi K, Yamada M, Hayasawa K, Kimura F, Motoyoshi K. 2000. $p56^{dok\text{-}2}$ as a cytokine-inducible inhibitor of cell proliferation and signal transduction. EMBO J 19:5114–5122.
Suzu S, Harada H, Matsumoto T, Okada S. 2005. HIV-1 Nef interferes with M-CSF receptor signaling through Hck activation and inhibits M-CSF bioactivities. Blood 105:3230–3237.
Trible RP, Emert-Sedlak L, Smithgall TE. 2006. HIV-1 Nef selecyively activates Src family kinases Hck, Lyn, and c-Src through SH3 domain interaction. J Biol Chem 281:27029–27038.
Ueno T, Motozono C, Dohki S, Mwimanzi P, Rauch S, Fackler OT, Oka S, Takiguchi M. 2008. CTL-mediated selective pressure influences dynamic evolution and pathogenetic functions of HIV-1 Nef. J Immunol 180:1107–1116.
van't Hof W, Resh MD, 1997. Rapid plasma membrane anchoring of newly synthesized p59fyn: Selective requirement for NH_2-terminal myristoylation and palmitoylation at cysteine-3. J Cell Biol 136:1023–1035.

ANTIMICROBIAL AGENTS AND CHEMOTHERAPY, July 2009, p. 2940–2948 Vol. 53, No. 7
0066-4804/09/$08.00+0 doi:10.1128/AAC.01727-08

The Novel CXCR4 Antagonist KRH-3955 Is an Orally Bioavailable and Extremely Potent Inhibitor of Human Immunodeficiency Virus Type 1 Infection: Comparative Studies with AMD3100[▽]

Tsutomu Murakami,[1]† Sei Kumakura,[2]† Toru Yamazaki,[2] Reiko Tanaka,[3] Makiko Hamatake,[1] Kazu Okuma,[3]‡ Wei Huang,[4] Jonathan Toma,[4] Jun Komano,[1] Mikiro Yanaka,[2]§ Yuetsu Tanaka,[3] and Naoki Yamamoto[1]*

AIDS Research Center, National Institute of Infectious Diseases, Tokyo 162-8640,[1] Biomedical Research Laboratories, Kureha Corporation, Tokyo 169-8503,[2] and Department of Immunology, Graduate School and Faculty of Medicine, University of the Ryukyus, Nakagami, Okinawa 903-0215,[3] Japan, and Monogram Biosciences, South San Francisco, California 94080[4]

Received 30 December 2008/Returned for modification 12 February 2009/Accepted 7 May 2009

The previously reported CXCR4 antagonist KRH-1636 was a potent and selective inhibitor of CXCR4-using (X4) human immunodeficiency virus type 1 (HIV-1) but could not be further developed as an anti-HIV-1 agent because of its poor oral bioavailability. Newly developed KRH-3955 is a KRH-1636 derivative that is bioavailable when administered orally with much more potent anti-HIV-1 activity than AMD3100 and KRH-1636. The compound very potently inhibits the replication of X4 HIV-1, including clinical isolates in activated peripheral blood mononuclear cells from different donors. It is also active against recombinant X4 HIV-1 containing resistance mutations in reverse transcriptase and protease and envelope with enfuvirtide resistance mutations. KRH-3955 inhibits both SDF-1α binding to CXCR4 and Ca^{2+} signaling through the receptor. KRH-3955 inhibits the binding of anti-CXCR4 monoclonal antibodies that recognize the first, second, or third extracellular loop of CXCR4. The compound shows an oral bioavailability of 25.6% in rats, and its oral administration blocks X4 HIV-1 replication in the human peripheral blood lymphocyte-severe combined immunodeficiency mouse system. Thus, KRH-3955 is a new promising agent for HIV-1 infection and AIDS.

The chemokine receptors CXCR4 and CCR5 serve as major coreceptors of human immunodeficiency virus type 1 (HIV-1), along with CD4 as a primary receptor for virus entry (2, 15, 18, 19). SDF-1α, which is a ligand for CXCR4, blocks the infection of CXCR4-utilizing X4 HIV-1 strains (7, 34). On the other hand, ligands for CCR5 such as RANTES inhibit CCR5-utilizing R5 HIV-1 (10). These findings made chemokines, chemokine derivatives, or small-molecule inhibitors of chemokine receptors attractive candidates as a new class of anti-HIV-1 agents. Many CCR5 antagonists have been developed as anti-HIV-1 drugs. These include TAK-779 (Takeda Pharmaceutical Company) (5), TAK-652 (6), TAK-220 (45), SCH-C (Schering-Plough) (43), SCH-D (vicriviroc) (42), GW873140 (aplaviroc; Ono Pharmaceutical/Glaxo Smith Kline) (28), and UK-427,857 (maraviroc; Pfizer Inc.) (17). Of these, maraviroc was approved by the U.S. FDA in 2007 for the treatment of R5 HIV-1 in treatment-experienced adult patients, combined with other antiretroviral treatment. Several classes of CXCR4 antagonists have also been reported. The bicyclam AMD3100 showed antivirus activity against many X4 and some R5X4 HIV strains in peripheral blood mononuclear cells (PBMCs) but not against R5 strains (16, 40). The pharmacokinetics and antiviral activity of this compound were also evaluated in humans (21, 22). T22, [Tyr-5,12, Lys-7]polyphemusin II, which is an 18-mer peptide derived from horseshoe crab blood cells, was reported to specifically inhibit X4 HIV-1 strains (30). Studies on the pharmacophore of T140 (a derivative of T22) led to the identification of cyclic pentapeptides (46).

In 2003, we reported that KRH-1636 is a potent and selective CXCR4 antagonist and inhibitor of X4 HIV-1 (23). Although the compound was absorbed efficiently from the rat duodenum, it has poor oral bioavailability. Continuous efforts to find more potent CXCR4 antagonists that are bioavailable when administered orally allowed us to develop KRH-3955 by a combination of chemical modification of the lead compound and biological assays. In this report, we describe the results of a preclinical evaluation of KRH-3955, including its in vitro anti-HIV-1 activity, its in vivo efficacy in the human peripheral blood lymphocyte (hu-PBL)-severe combined immunodeficiency (SCID) mouse model, and its pharmacokinetics in rats in comparison with those of AMD3100.

* Corresponding author. Mailing address: AIDS Research Center, National Institute of Infectious Diseases, 1-23-1 Toyama, Shinjuku-ku, Tokyo 162-8640, Japan. Phone: 81-3-5285-1111, ext. 2302. Fax: 81-3-5285-1165. E-mail: nyama@nih.go.jp.

† T.M. and S.K. contributed equally to this work.

‡ Present address: Department of Safety Research on Blood and Biological Products, National Institute of Infectious Diseases, Gakuen 4-7-1, Musashimurayama-shi, Tokyo 208-0011, Japan.

§ Present address: Kureha Special Laboratory Co., Ltd., Fukushima 974-8232, Japan.

▽ Published ahead of print on 18 May 2009.

MATERIALS AND METHODS

Compounds. The synthesis and purification of KRH-3955, *N,N*-dipropyl-*N'*-[4-({[(1*H*-imidazol-2-yl)methyl][(1-methyl-1*H*-imidazol-2-yl)methyl]amino}methyl)benzyl]-*N'*-methylbutane-1,4-diamine tri-(2*R*,3*R*)-tartrate, were carried out by Kureha Corporation. The chemical structure of KRH-3955 is shown in Fig. 1. The CXCR4 antagonist AMD3100 and zidovudine (AZT) were obtained from Sigma. Saquinavir was obtained

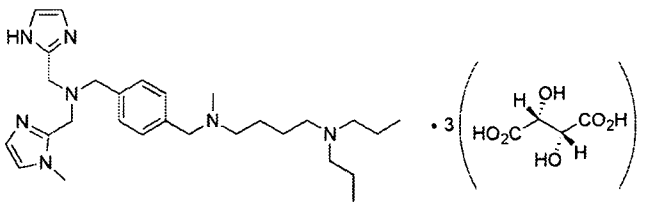

FIG. 1. Chemical structure of KRH-3955.

from the NIH AIDS Research and Reference Reagent Program, NIAID, Bethesda, MD. AMD070 and SCH-D were synthesized at Kureha Corporation.

Cells. Molt-4 no. 8 cells (24) were maintained in RPMI 1640 medium (Invitrogen, Carlsbad, CA) supplemented with 10% fetal bovine serum (Sigma, St. Louis, MO) and antibiotics (50 ng/ml penicillin, 50 ng/ml streptomycin, and 100 ng/ml neomycin; Invitrogen), which is referred to as RPMI medium. Chemokine receptor-expressing human embryonic kidney 293 (HEK293) cells (ATCC CRL-1573) and Chinese hamster ovary (CHO) cells (ATCC CCL-61) were maintained in minimal essential medium or F-12 (Invitrogen) supplemented with 10% fetal bovine serum and antibiotics (50 ng/ml penicillin, 50 ng/ml streptomycin, and 100 ng/ml neomycin). PBMCs from HIV-1-seronegative healthy donors were isolated by Ficoll-Hypaque density gradient (Lymphosepal; IBL, Gunma, Japan) centrifugation (31) and grown in RPMI medium supplemented with recombinant human interleukin-2 (rhIL-2; Roche, Mannheim, Germany) at 50 U/ml.

Viruses. Viral stocks of HIV-1_{NL4-3}, HIV-1_{JR-CSF}, and HIV-$1_{89.6}$ were each produced in the 293T cell line by transfection with HIV-1 molecular clone plasmids pNL4-3 (1), pYK-JRCSF (25), and p89.6 (11), respectively, by the calcium phosphate method. The 50% tissue culture infective dose was determined by an end-point assay with PBMC cultures activated with immobilized anti-CD3 monoclonal antibody (MAb) (33, 51). Subtype B HIV-1 primary isolates 92HT593, 92HT599 (N. Hasley), and 91US005 (B. Hahn) and AZT-resistant HIV-1 (A018) (D. D. Richman) (26) were obtained from the AIDS Research and Reference Reagent Program, Division of AIDS, NIAID, NIH. These clinical isolates were propagated in the activated PBMCs prepared as described above.

Anti-HIV-1 assays. Human PBMCs activated with immobilized anti-CD3 MAb (OKT-3; ATCC, Manassas, VA) in RPMI medium for 3 days were infected with various HIV-1 strains, including primary clinical isolates, at a multiplicity of infection of 0.001. After 3 h of adsorption, the cells were washed and cultured in RPMI medium supplemented with rhIL-2 (50 U/ml) in the presence or absence of the test compounds. Amounts of HIV-1 capsid (p24) antigen produced in the culture supernatants were measured by an enzyme-linked immunosorbent assay kit (ZeptoMetrix Corp., Buffalo, NY) 7 to 10 days after infection. The cytotoxicities of the compounds were tested on the basis of the viability and proliferation of the activated PBMCs, as determined with Cell Proliferation Kit II (XTT) from Roche (36).

Susceptibility of multidrug-resistant HIV-1 to CXCR4 antagonists was also measured by using recombinant viruses in a single replication cycle assay (9, 49). HIV-1 resistance test vectors (RTVs) contain the entire protease (PR) coding region and the reverse transcriptase (RT) coding region, from amino acid 1 to amino acid 305, amplified from patient plasma and a luciferase expression cassette inserted in the *env* region. The RTVs in this study contain patient-derived PR and RT sequences that possess mutations associated with resistance to PR, RT, or both PR and RT. Env-pseudotyped viruses were produced by cotransfecting 293 cells with RTV plasmids and expression vectors encoding the Env protein of well-characterized X4-tropic laboratory strain HXB2, NL4-3, or NL4-3 containing the Q40H enfuvirtide (T20) resistance mutation introduced by site-direct mutagenesis. The virus stocks were harvested 2 days after transfection and used to infect U87 $CD4^+$ cells (kind gifted from N. Landau, NYU School of Medicine) expressing CXCR4 in 96-well plates, with serial dilutions of CXCR4 antagonists. Target cells were lysed, and luciferase activity was measured to assess virus replication in the presence and absence of inhibitors. Drug concentrations required to inhibit virus replication by 50% (IC_{50}) were calculated.

Immunofluorescence. Molt-4 cells or CXCR4-expressing HEK293 cells were treated with various concentrations of KRH-3955 or AMD3100 in RPMI medium or phosphate-buffered saline containing 1% bovine serum albumin and 0.05% NaN_3 (fluorescence-activated cell sorting [FACS] buffer). In washing experiments, cells were washed with RPMI medium or FACS buffer. The cells were Fc blocked with 2 mg/ml normal human immunoglobulin G (IgG) in FACS buffer and then stained directly with mouse MAbs 12G5-phycoerythrin (PE) and 44717-PE (R&D Systems, Inc., Minneapolis, MN) or rat MAb A145-fluorescein isothiocyanate (FITC) and indirectly with MAb A80. The A145 and A80 MAbs were produced in ascitic fluid of BALB/c nude mice, and IgG fractions were obtained from ascitic fluid by gel filtration chromatography with Superdex G200 (Amersham Pharmacia). Goat anti-rat IgG (heavy and light chains) labeled with FITC was purchased from American Corlex (47). After washing, the cells were analyzed on a FACScalibur (BD Biosciences, San Jose, CA) flow cytometer with CellQuest software (BD Biosciences).

DNA construction and transfection. Chemokine receptor-expressing CHO cells were generated as reported previously (23). Human CXCR4 cDNA was cloned into the pcDNA3.1 vector. Mutations were introduced by using the QuikChange II site-directed mutagenesis kit (Stratagene, La Jolla, CA). All constructs were verified by DNA sequencing and transfected into 293 cells by using the Lipofectamine reagent (Invitrogen) (48). Stable transfectants were selected in the presence of 400 μg/ml G418 (Invitrogen). The COOH-terminal intracellular domain of CXCR4 (residues 308 to 352) was deleted in all mutants and the wild type. This deletion has no influence on HIV-1 infection or on SDF-1α binding and signaling but abolishes ligand-induced endocytosis (3).

Ligand-binding assays. Chemokine receptor-expressing CHO cells (5×10^6/0.2 ml per well) were cultured in a 24-well microtiter plate. After 24 h of incubation at 37°C, the culture medium was replaced with binding buffer (RPMI medium supplemented with 0.1% bovine serum albumin). Binding reactions were performed on ice in the presence of ^{125}I-labeled chemokines (final concentration of 100 pmol/liter; PeproTech Inc., Rocky Hill, NJ) and various concentrations of test compounds. After washing away of unbound ligand, cell-associated radioactivity was counted with a scintillation counter as described previously (23).

CXCR4-mediated Ca^{2+} signaling. Fura2-acetoxymethyl ester (Dojindo Laboratories, Kumamoto, Japan)-loaded CXCR4-expressing CHO cells were incubated in the absence or presence of various concentrations of KRH-3955 or AMD3100. Changes in intracellular Ca^{2+} levels in response to SDF-1α (1 μg/ml) were determined by using a fluorescence spectrophotometer as described previously (30).

Detection of KRH-3955 in blood after oral administration. The plasma concentration-time profile of R-176211 (distilled water was used as a vehicle), the free form of KRH-3955, was examined after a single oral administration of KRH-3955 at a dose of 10 mg/kg or intravenous administration at a dose of 10 mg/kg to male Sprague-Dawley rats (CLEA, Kanagawa, Japan). R-176211 in plasma was measured by liquid chromatography-tandem mass spectrometry. Pharmacokinetic parameters were calculated by using WinNonlin Professional (ver. 3.1; Pharsight Co.).

Infection of hu-PBL–SCID mice. Two groups of C.B-17 SCID mice (CLEA, Kanagawa, Japan) were administered a single dose of either KRH-3955 or tartrate (2% glucose solution was used as the vehicle) as a control orally (p.o.) and fed for 2 weeks. These mice were then engrafted with human PBMCs (1×10^7 cells/animal intraperitoneally [i.p.]) and after 1 day were infected i.p. with 1,000 infective units of X4 HIV-1_{NL4-3}. IL-4 (2 μg per animal) was administrated i.p. on days 0 and 1 after PBMC engraftment to enhance X4 HIV-1 infection. After 7 days, human lymphocytes were collected from the peritoneal cavities and spleens of the infected mice and cultured in vitro for 4 days in RPMI medium supplemented with 20 U/ml rhIL-2. HIV-1 infection was monitored by measuring p24 levels in the culture supernatant. We used a selected donor whose PBMCs could be engrafted at an efficiency of >80% in C.B-17 SCID mice. Usually, 5×10^5 to 10×10^5 human $CD4^+$ T cells can be recovered from each hu-PBL–SCID mouse. Mice with no or low recovery of human $CD4^+$ T cells at the time of analysis were omitted. For ex vivo cultures, we used a quarter of the cells recovered from a mouse. The protocols for the care and use of the hu-PBL–SCID mice were approved by the Committee on Animal Research of the University of the Ryukyus before initiation of the present study.

RESULTS

Anti-HIV-1 activities of KRH-3955 in activated PBMCs. The inhibitory activity of KRH-3955 against X4 HIV-1 (NL4-3), R5X4 HIV-1 (89.6), and R5 HIV-1 (JR-CSF) was examined in activated human PBMCs from two different donors. KRH-3955 inhibited the replication of both X4 and R5X4 HIV-1 in activated PBMCs with 50% effective concentrations (EC_{50}) of 0.3 to 1.0 nM but did not affect R5 HIV-1 replication, even at concentration of up to 200 nM (Table 1). In contrast, the CCR5 antagonist SCH-D (vicriviroc) inhibited R5 HIV-1 rep-

TABLE 1. Anti-HIV-1 activity of KRH-3955 in activated PBMCs[a]

Virus	Donor	EC_{50} (nM)[b]					
		KRH-3955	AMD3100	AMD070	SCH-D	AZT	SQV
NL4-3	A	1.1	41	35	>1,000	11	9.0
X4	B	0.33	15	15	>1,000	8.0	29
89.6	A	0.38	44	55	>1,000	7.4	9.9
R5X4	B	ND[c]	ND	ND	ND	ND	ND
JR-CSF	A	>200	>200	>200	0.37	0.96	2.6
R5	B	>200	>200	>200	1.2	6.2	8.0
A018H (X4) (pre-AZT)	C	1.4	38	ND	ND	1.9	ND
A018G (X4) (post-AZT)	C	1.3	32	ND	ND	87,000	ND

[a] PBMCs from two different donors were used in each assay. Anti-HIV-1 activity was determined by measuring the p24 antigen level in culture supernatants.
[b] Assays were carried out in triplicate wells. The average of two to four experiments is shown.
[c] ND, not determined.

lication but inhibited neither X4 nor R5X4 HIV-1 replication (Table 1). The anti-HIV activity of KRH-3955 against the 89.6 virus from donor B was not determined because the virus did not replicate enough for calculation of the anti-HIV activity of KRH-3955 and other drugs. Notably, the anti-HIV-1 activity of KRH-3955 was much higher than that of AMD3100, a well-known X4 HIV-1 inhibitor, or AMD070, the other X4 inhibitor that is bioavailable when administered orally. KRH-3955 also inhibited the replication of clinical isolates of X4 HIV-1 (92HT599) and R5X4 HIV-1 (92HT593) with EC_{50} ranging from 4.0 to 4.2 nM (data not shown). Although both KRH-3955 and AMD3100 were effective against at least some R5X4 HIV-1 strains in activated PBMCs, neither KRH-3955 nor AMD3100 inhibited the infection of CD4/CCR5 cells by R5 or R5X4 HIV-1, even at a concentration of 1,660 nM (data not shown). Importantly, the 50% cytotoxic concentration of KRH-3955 in activated PBMCs (donor A) was 57 μM, giving a high therapeutic index (51,818) in the case of NL4-3 infection, which was higher than that of AZT (8,000 in the case of donor A). These results indicate that the compound is a selective inhibitor of HIV-1 that can utilize CXCR4 as a coreceptor. Since a CXCR4 antagonist should be used in combination with a CCR5 antagonist in a clinical setting, we next examined whether the combined use of both antagonists efficiently blocks mixed infection with X4 and R5 HIV-1. Combination of KRH-3955 and SCH-D at 4 plus 4 nM and 20 plus 20 nM blocked the replication of 50:50 mixtures of NL4-3 and JR-CSF by 91 and 96%, respectively (data not shown). Thus, KRH-3955 is a highly potent and selective inhibitor of X4 HIV-1.

Anti-HIV-1 activities of KRH-3955 in activated PBMCs from different donors. It has been observed that the anti-HIV-1 activity of compounds in PBMCs varies from donor to donor. Therefore, the anti-HIV-1 activity of KRH-3955 against X4 HIV-1 was examined in activated PBMCs from eight different donors. The levels of p24 antigen in NL4-3-infected cultures ranged from 17 to 120 ng/ml (Table 2). KRH-3955 inhibited the replication of NL4-3 with EC_{50} ranging from 0.23 to 1.3 nM and with EC_{90} ranging from 2.7 to 3.5 nM (Table 2), demonstrating that the anti-HIV-1 activity of KRH-3955 was independent of the PBMC donor.

Anti-HIV-1 activities of KRH-3955 against drug-resistant HIV-1 strains. To further assess the efficacy of KRH-3955, we used a single-cycle assay to evaluate the activity of KRH-3955 against a panel of recombinant viruses that express an X4-tropic envelope protein (HXB2) but contain PR and RT sequences containing a wide variety of mutations associated with resistance to PR inhibitors (PIs), nucleoside RT inhibitors (NRTIs), and non-NRTIs (NNRTIs). This assessment was also performed with recombinant viruses that express an X4-tropic envelope protein (NL4-3) that contains the Q40H mutation and displays resistance to T20 (an entry inhibitor). The results of these experiments demonstrate that both KRH-3955 and AMD3100 inhibited the infection of CD4/CXCR4 cells by these recombinant drug-resistant viruses, including viruses resistant to PIs, NRTIs, or NNRTIs; multidrug-resistant viruses; and T20-resistant viruses (Table 3). We also observed that KRH-3955 inhibited the replication of A018G, a highly AZT-resistant strain, in activated PBMCs with an EC_{50} of 1.3 nM (Table 1).

KRH-3955 selectively inhibits ligand binding to CXCR4. To investigate whether KRH-3955 specifically blocks ligand binding to CXCR4, the inhibitory effect of the compound on chemokine binding to CHO cells expressing CXCR4, CXCR1, CCR2b, CCR3, CCR4, or CCR5 was determined. KRH-3955 efficiently inhibited SDF-1α binding to CXCR4 in a dose-dependent manner (Fig. 2 and 3b), and the IC_{50} for SDF-1α binding was 0.61 nM, which is similar to its EC_{50} against HIV-1. Similar results were obtained when we used a Molt-4 T cell line as the CXCR4-expressing target cell (Fig. 3a). Interestingly, the inhibitory activity of AMD3100 against SDF-1α binding was much weaker than its anti-HIV-1 activity (Fig. 3), suggesting that the binding sites of these two compounds are different. In contrast, the compound did not affect the binding

TABLE 2. Anti-HIV-1 activity of KRH-3955 against NL4-3 infection of PBMCs from eight different donors

Donor	p24 level (ng/ml)	EC_{50} (nM)	EC_{90} (nM)
1	31	1.30	3.2
2	25	1.20	3.2
3	17	1.20	3.3
4	40	0.70	2.9
5	120	0.77	2.9
6	58	1.50	3.5
7	49	0.23	2.7
8	53	1.00	3.0
Mean ± SD	49 ± 32	0.99 ± 0.40	3.1 ± 0.30

TABLE 3. KRH-3955 susceptibilities of drug-resistant viruses[a]

Virus[b]	IC_{50} (nM)[c]	
	KRH-3955	AMD3100
NL4-3	0.50	4.6
HXB2	0.60	6.2
NRTI-Res (HXB2-env)	0.60	9.0
NNRTI-Res (HXB2-env)	0.80	7.0
PI-Res (HXB2-env)	0.70	9.2
MDR (HXB2-env)	0.70	5.3
T20-Res (NL4-3-env)	0.40	2.3

[a] Susceptibility of drug-resistant HIV-1 was measured by using a single-cycle recombinant virus assay (see Materials and Methods).
[b] The pseudoviruses containing X4-tropic envelope (HXB2 or NL4-3) and patient-derived PR and RT sequences containing mutations associated with resistance to PR (PI-Res), RT (NRTI-Res or NNRTI-Res), or both (MDR) (the mutations are not shown). T20-Res contains a site-directed mutation (Q40H) in the NL4-3 envelope.
[c] IC50, 50% inhibitory concentration of CXCR4 antagonists.

of ^{125}I-labeled SDF-1α, ^{125}I-labeled RANTES, ^{125}I-labeled MCP-1, ^{125}I-labeled TARC, ^{125}I-labeled RANTES, or ^{125}I-labeled IL-8 to CXCR4, CCR1, CCR2b, CCR4, CCR5, or CXCR1, respectively (Fig. 2). Thus, KRH-3955 selectively blocks the binding of SDF-1α to CXCR4.

KRH-3955 exhibits inhibition of Ca^{2+} signaling through CXCR4. We next examined whether KRH-3955 acts as an agonist or antagonist of CXCR4 by using CXCR4-expressing CHO cells. The addition of KRH-3955 inhibited the SDF-1α-induced increase in the intracellular Ca^{2+} concentration in a dose-dependent manner, whereas 100 nM AMD3100 did not affect Ca^{2+} mobilization (Fig. 4). KRH-3955 itself did not affect Ca^{2+} mobilization at up to 1 μM (data not shown). We performed the Ca^{2+} mobilization assay with human PBMCs but could not detect an SDF-1α-induced Ca^{2+} signal mainly due to low expression of CXCR4 (data not shown). Thus, KRH-3955 inhibits Ca^{2+} signaling through CXCR4.

Effect of KRH-3955 on anti-CXCR4 antibody binding to CXCR4-expressing cells. To localize the binding site(s) of KRH-3955, the effects of KRH-3955 and AMD3100 on the binding of four types of anti-CXCR4 MABs were first examined. We used MAbs A145, 12G5, 44717, and A80, which are specific for the N terminus, extracellular loop 1 (ECL1) and ECL2, ECL2, and ECL3, respectively. Neither KRH-3955 nor AMD3100 inhibited A145 binding to CXCR4-expressing Molt-4 cells (Fig. 5). Both compounds inhibited the binding of MAbs 12G5, 44717, and A80 to Molt-4 cells in a dose-depen-

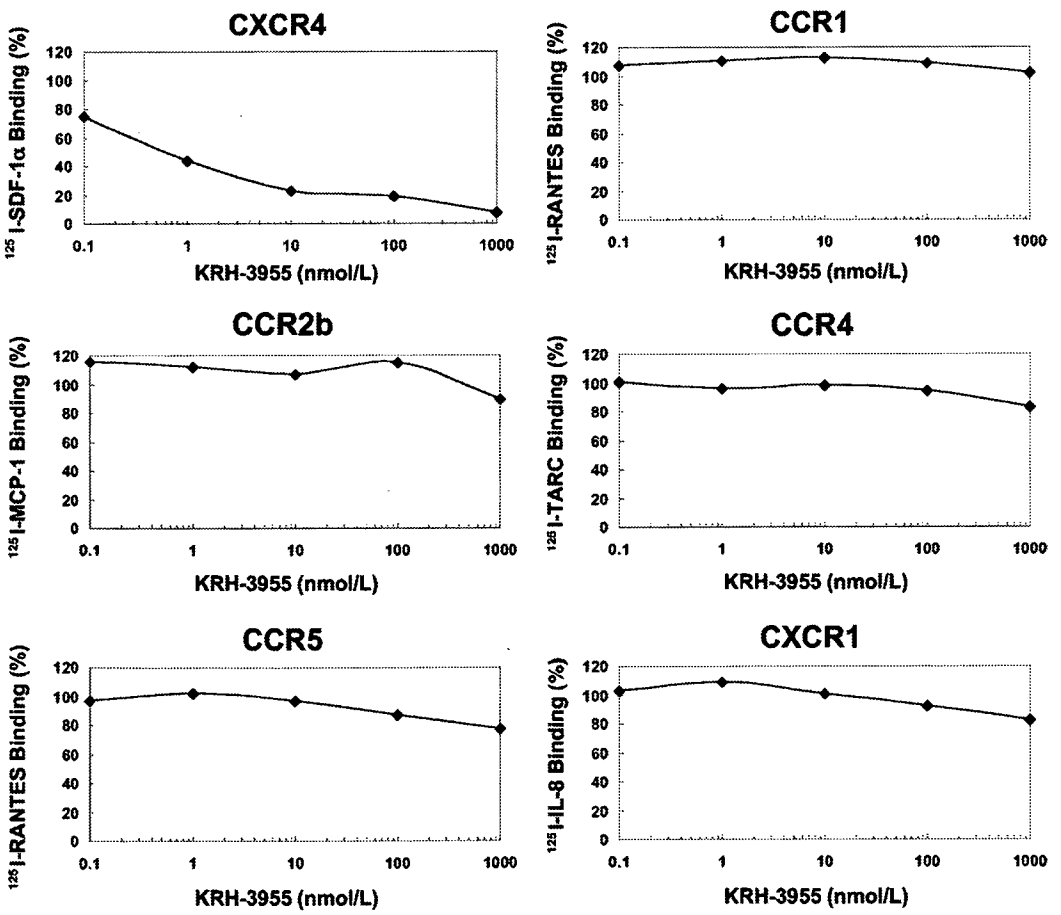

FIG. 2. Inhibitory effects of KRH-3955 on chemokine binding to CXCR4-, CCR1-, CCR2b-, CCR4-, CCR5-, or CXCR1-expressing CHO cells. Chemokine receptor-expressing CHO cells were incubated with various concentrations of KRH-3955 in binding buffer containing ^{125}I-labeled chemokine. Binding reactions were performed on ice and were terminated by washing out the unbound ligand. Cell-associated radioactivity was measured with a scintillation counter. Percent binding was calculated as 100 × [(binding with inhibitor − nonspecific binding)/(binding without inhibitor − nonspecific binding)]. The data represent the means in duplicate wells in a single experiment.

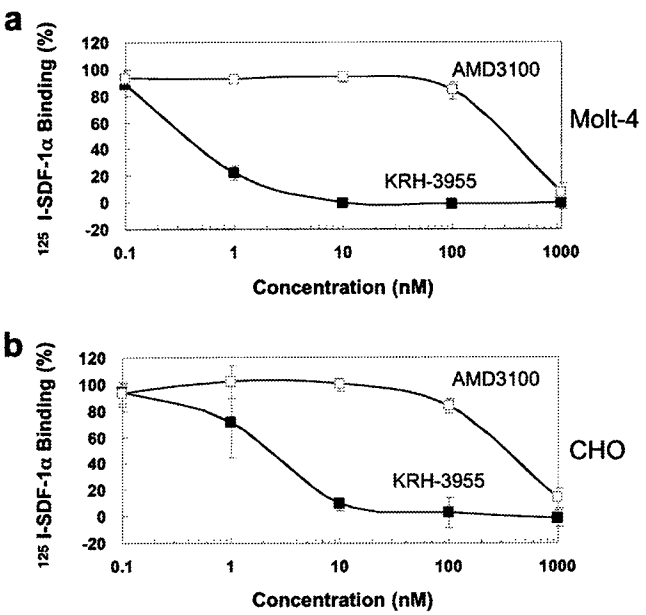

FIG. 3. Concentration-dependent inhibition by KRH-3955 of SDF-1α binding to (a) Molt-4 and (b) CXCR4-expressing CHO cells. CXCR4-expressing CHO cells were incubated with various concentrations of KRH-3955 (■) or AMD3100 (□) in binding buffer containing ^{125}I-labeled SDF-1α. Binding reactions were performed, and percent binding was calculated as described in the legend to Fig. 2. The data represent the means ± standard deviations of three independent experiments.

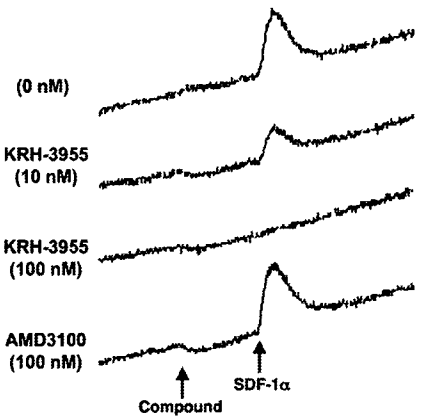

FIG. 4. Inhibitory effects of KRH-3955 on SDF-1α-induced Ca^{2+} mobilization in CXCR4-expressing CHO cells. Fura-2-acetoxymethyl ester-loaded CXCR4-expressing CHO cells were incubated in the presence or absence of various concentrations of KRH-3955 or AMD3100. Changes in intracellular Ca^{2+} levels in response to SDF-1α (1 μg/ml) were determined with a fluorescence spectrophotometer. The data show representative data for two independent experiments.

dent manner. The inhibitory activity of KRH-3955 is similar to its anti-HIV-1 activity, whereas the inhibitory activity of AMD3100 is much weaker than its anti-HIV-1 activity. Similar data were obtained when activated human PBMCs were used as target cells (data not shown). KRH-3955 itself did not induce internalization of CXCR4 at concentrations of up to 1 μM (data not shown), as KRH-1636 did (23). These results suggest that the binding sites of KRH-3955 are located in a region composed of all three ECLs of CXCR4.

Long-lasting inhibitory effects of KRH-3955 on the binding of MAb 12G5. The inhibitory effect of KRH-3955 on the binding of MAb 12G5 was examined with or without washing of the compound from the cells. Molt-4 cells were treated with 10 nM KRH-3955 or 1,000 nM AMD3100 for 15 min. With or without washing, the cells were stained with MAb 12G5-PE and the amount of bound antibody was analyzed by flow cytometry. KRH-3955 strongly inhibited MAb 12G5 binding to Molt-4 cells irrespectively of washing (Fig. 6a). In contrast, AMD3100 efficiently inhibited MAb 12G5 binding without washing away of the compound but lost its inhibitory activity after washing away of the compound (Fig. 6a). The long-lasting inhibitory effect of KRH-3955 on the binding of MAb 12G5 was further tested. Molt-4 cells were preincubated with or without KRH-3955 at 10 nM. The compound was washed away, and the cells were further incubated at 37°C in compound-free growth medium. At 0, 3, and 6 h after compound removal, the cells were stained with MAb 12G5-PE and analyzed by flow cytometry. Even at 6 h after washing away of the compound, KRH-3955 inhibited MAb 12G5 binding by approximately 40% (Fig. 6b). These results suggest that KRH-3955 has a strong binding affinity for CXCR4 and a slow dissociation rate, although competition assays with the two molecules (KRH-3955 versus MAb 12G5 with radioactive, nonradioactive, or different labeling) are necessary to provide definitive conclusions.

Inhibition of MAb 12G5 binding to CXCR4 mutants by KRH-3955. The effects of different CXCR4 mutations on the inhibitory activity of KRH-3955 against MAb 12G5 binding to CXCR4 were examined. HEK293-CXCR4 transfectants were preincubated with various concentrations of KRH-3955 and AMD3100, after which the compound was washed away. The binding of PE-conjugated MAb 12G5 was measured by flow cytometry. As reported previously, AMD3100 substantially lost its blocking activity against MAb 12G5 binding for D171A (TM4), D262A (TM6), and E288A/L290A (TM7) mutants, as shown by previous reports (Table 4) (20, 37, 38). In contrast, the blocking activity of KRH-3955 against MAb 12G5 binding was not affected by the above mutations. In contrast, the H281A (ECL3) mutant displayed decreased inhibition of MAb 12G5 binding by KRH-3955 (Table 4). These data further support the hypothesis that the CXCR4 interaction sites of KRH-3955 are different from those of AMD3100.

Pharmacokinetic studies of KRH-3955 in rats. In pharmacokinetics studies, KRH-3955 was orally or intravenously administrated to Sprague-Dawley rats at a dose of 10 mg/kg. The plasma concentration of R-176211, the free form of KRH-3955, was monitored by liquid chromatography-tandem mass spectrometry. In these studies, KRH-3955 was found to be well absorbed and the absolute oral bioavailability in rats was calculated to be 25.6% based on the area under the plasma concentration-time curve (Table 5). However, KRH-3955 also showed a long elimination half-life after single-dose administration to rats, suggesting long-term accumulation of the compound in tissues (Table 5). KRH-3955 was found to be stable in human hepatic microsomes, and no significant inhibition of CYP450 liver enzymes by this compound was observed (data

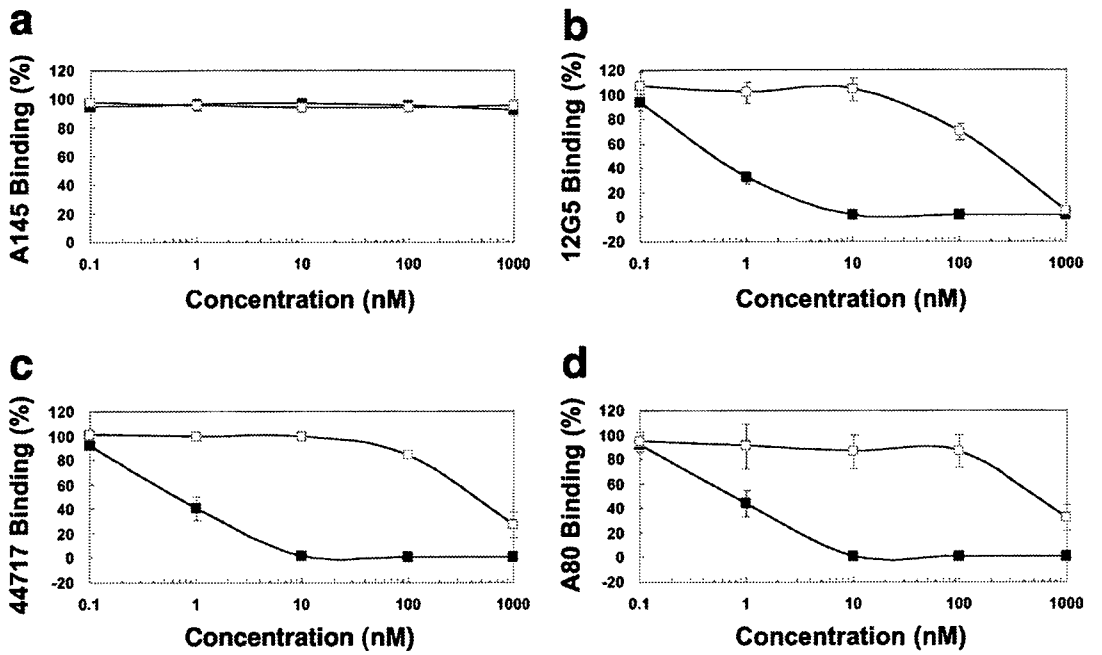

FIG. 5. Effect of KRH-3955 on the binding of four different MAbs to the CXCR4 receptor. Molt-4 cells were incubated with various concentrations of KRH-3955 (■) or AMD3100 (□). The cells were stained directly with MAbs 12G5 (recognizes ECL1 and ECL2 of CXCR4)-PE, 44717 (recognizes ECL2 of CXCR4)-PE, and A145 (recognizes the N terminus of CXCR4)-FITC or indirectly with MAb A80 (recognizes ECL3 of CXCR4). The mean fluorescence of the stained cells was analyzed with a FACScalibur flow cytometer. Percent binding was calculated with the equation described in the legend to Fig. 2. The data represent the means ± standard deviations of three independent experiments.

not shown). Thus, orally administered KRH-3955 is bioavailable in rats.

KRH-3955 efficiently suppresses X4 HIV-1 infection in hu-PBL–SCID mice. We then examined whether KRH-3955 can interfere with X4 HIV-1 infection in vivo by using hu-PBL–SCID mice. Mice were administrated a single dose (10 mg/kg) of either KRH-3955 or tartrate (as a control) p.o. and fed for 2 weeks. These mice were then engrafted with human PBMCs, and after 1 day, these "humanized" mice were infected with infectious X4 HIV-1 (NL4-3). After 7 days, human lymphocytes harvested from the peritoneal cavities and spleens of the infected mice were cultured for 4 days in vitro in the presence of rhIL-2 in order to determine the level of HIV-1 infection by the p24 enzyme-linked immunosorbent assay. The maximum concentration of KRH-3955 in blood after p.o. administration was estimated to be 100 nM (data now shown). Under these conditions, four of five mock-treated mice were infected whereas only one of five mice treated with KRH-3955 was infected (Table 6). The one infected mouse in the KRH-3955-treated group (no. 5)

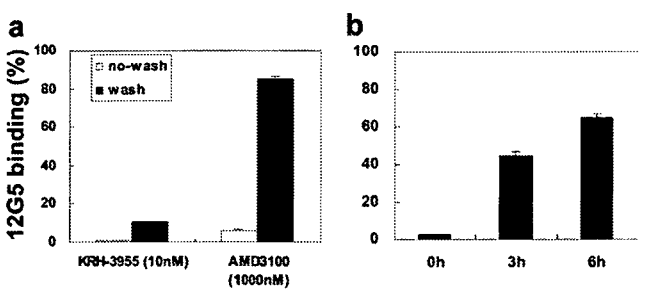

FIG. 6. Long-lasting inhibitory effects of KRH-3955 on the binding of MAb 12G5. (a) Molt-4 cells were treated with 10 nM KRH-3955 or 1,000 nM AMD3100 for 15 min. With (■) or without (□) washing, the cells were staining with MAb 12G5-PE and analyzed by flow cytometry. (b) Long-lasting inhibitory effect of KRH-3955 on the binding of MAb 12G5. Molt-4 cells were preincubated with or without KRH-3955 at 10 nM. The compound was washed away, and the cells were further incubated at 37°C in compound-free RPMI medium. At 0, 3, and 6 h after removal of the compound, the cells were staining with MAb 12G5-PE and analyzed by flow cytometry. The data represent the means of triplicate wells in a single experiment.

TABLE 4. Affinity of KRH-3955 and AMD3100 for wild-type CXCR4 and various mutant forms of CXCR4[a]

CXCR4 (location)	KRH-3955		AMD3100	
	IC_{50}	IC_{90}	IC_{50}	IC_{90}
Wild type	2.8 ± 0.5	8.2 ± 0.4	289.1 ± 25.5	971.1 ± 31.2
V99A (ECL1)	1.5 ± 0.2	7.4 ± 0.2	258.5 ± 25.9	>1,000
V112A (TM3)	2.2 ± 0.2	>10	196.6 ± 28.5	821.3 ± 15.4
H113A (TM3)	0.8 ± 0.3	6.3 ± 0.2	296.4 ± 112.2	>1,000
D171A (TM4)	3.2 ± 0.1	>10	>1,000	>1,000
D181A (ECL2)	0.5 ± 0.1	5.1 ± 0.3	143.7 ± 29.3	795.6 ± 79.9
H203A (TM5)	0.5 ± 0.1	5.3 ± 0.1	259.0 ± 11.5	860.6 ± 22.4
D262A (TM6)	1.6 ± 0.3	8.1 ± 0.5	>1,000	>1,000
E275A (ECL3)	1.0 ± 0.2	6.4 ± 0.1	235.6 ± 30.2	930.2 ± 26.1
E277A (ECL3)	3.1 ± 0.1	8.7 ± 0.1	469.5 ± 19.2	>1,000
V280A (ECL3)	1.0 ± 0.2	6.1 ± 0.1	175.3 ± 10.3	821.2 ± 47.3
H281A (ECL3)	14.1 ± 5.2	248.3 ± 74.9	72.7 ± 42.9	572.2 ± 118.1
W283A (ECL3)	1.3 ± 0.2	6.9 ± 0.2	300.2 ± 10.5	>1,000
I284A (TM7)	1.2 ± 0.2	6.8 ± 0.5	265.8 ± 20.8	>1,000
E288A/L290A (TM7)	1.6 ± 0.1	7.7 ± 0.3	>1,000	>1,000

[a] The data shown, which represent means ± SDs (n = 3) of nanomolar concentrations, were obtained from competition binding on HEK293 cells expressing the wild-type or mutant CXCR4 receptors with MAb 12G5.

TABLE 5. Pharmacokinetic parameters of KRH-3955 after single oral administration in rats[a]

Parameter	Value when given i.v. or p.o. at 10 mg/kg
Bioavailability (%)[b]	25.6
I.v. half-life (h)	99.0 ± 13.1
I.v. CL (liters/h/kg)[c]	3.9 ± 0.07
V_1 (ss) (liters/kg)[d]	374.0 ± 14
P.o. C_{max} (ng/ml)[e]	86.3 ± 23.6
T_{max} (h)[f]	2.3 ± 1.53
P.o. AUC_{0-336} (ng · h/ml)[g]	325.0 ± 38

[a] The data shown are means ± SDs (n = 3).
[b] Bioavailability = $(AUC_{oral}/AUC_{i.v.}) \times (dose_{i.v.}/dose_{oral}) \times 100$.
[c] CL, clearance.
[d] V_1 (ss), volume of distribution in central compartment at steady state.
[e] C_{max}, maximum concentration of drug in serum.
[f] T_{max}, time to maximum concentration of drug in serum.
[g] AUC_{0-336}, area under the plasma concentration-time curve from time zero to 336 h.

TABLE 6. Inhibition of infection of hu-PBL–SCID mice with X4 HIV-1 by KRH-3955[a]

Group and mouse no.	p24 produced (pg/ml)
Control	
1	747
2	10,263
3	<5
4	5,821
5	1,902
KRH-3955	
6	<5
7	<5
8	<5
9	<5
10	36

[a] Two groups of C.B-17 SCID mice (n = 5) were administrated a single dose of either KRH-3955 or tartrate (as a control) p.o. and fed for 2 weeks. These mice were then engrafted with human PBMCs (1×10^7 per animal i.p.), and after 1 day, these "humanized" mice were infected with 1,000 infective units of X4 HIV-1_{NL4-3}. IL-4 (2 mg per animal) was administrated i.p. on days 0 and 1 after PBMC engraftment to enhance X4 HIV-1 infection. After 7 days, human lymphocytes were harvested from the infected mice and cultured in vitro for 4 days in medium containing 20 U/ml IL-2. HIV-1 infection was monitored by measuring p24 levels. Means from duplicate determinations are shown. <5, below detection level.

showed low levels of p24 production. These results indicate that single-dose p.o. administration of KRH-3955 was very effective in protecting against X4 HIV-1 infection in an in vivo mouse model.

DISCUSSION

In this study, we clearly demonstrate that KRH-3955, a KRH-1636 derivative that is bioavailable when administered orally, is a potent inhibitor of HIV-1 infection both in vitro and in vivo. KRH-3955 selectively inhibited X4 HIV-1 strains, including clinical isolates, as we have previously shown with KRH-1636. Furthermore, KRH-3955 is approximately 40 times more potent than KRH-1636 in its anti-HIV-1 activity in activated PBMCs (Table 1). The anti-HIV-1 activity of KRH-3955 was independent of the PBMC donor (Table 2). KRH-3955 also inhibited the infectivity of recombinant viruses resistant to NRTIs, NNRTIs, PIs, and T20 (Table 3). Pharmacokinetic studies of KRH-3955 indicated that the compound is bioavailable in rats when administered orally (Table 5). In addition, oral administration of the compound efficiently inhibited the replication of X4 HIV-1 in the hu-PBL–SCID mouse model (Table 6). Although we could show that KRH-3955 is a potent inhibitor of subtype B HIV-1 isolates, we need to examine the efficacy of this compound against non-subtype B HIV-1 isolates because of the global nature of the HIV/AIDS epidemic and the regional diversity of HIV-1 subtypes.

R5 HIV-1 is isolated predominantly during the acute and asymptomatic stage (12) and is also believed to be important for virus transmission between individuals. In contrast, X4 HIV-1 strains emerge in approximately 50% of infected individuals and their emergence is associated with a rapid $CD4^+$ T-cell decline and disease progression (35, 50). One recent report also indicated that detection of X4 HIV-1 at baseline independently predicted disease progression (13), although it is still not known whether the emergence of X4 HIV-1 is a cause or outcome of disease progression. These findings strongly support the need for highly potent CXCR4 inhibitors that are bioavailable when administered orally such as KRH-3955.

Inhibition of ligand binding to chemokine receptors by KRH-3955 was specific for CXCR4 (Fig. 2), as we observed previously for KRH-1636. This specific inhibition of SDF-1α binding to CXCR4 by KRH-3955 is absolutely necessary for developing an anti-HIV agent to avoid immune dysregulation by nonspecific inhibition of binding by other chemokines. It is of note that the inhibitory activity of the compound against SDF-1α binding is similar to that against HIV-1 infection, which is different from that of control compound AMD3100. Where on the CXCR4 molecule is the binding site(s) of KRH-3955? Experiments to examine the effect of KRH-3955 on the binding of several anti-CXCR4 MAbs suggest that the binding sites of KRH-3955 are located in all three ECLs of CXCR4 (Fig. 5). To further define the binding site(s) of KRH-3955, we examined the effects of CXCR4 point mutations on the inhibitory activity of KRH-3955 against MAb 12G5 binding to the receptor. AMD3100 was used as a control. The inhibitory activity of AMD3100 against MAb 12G5 binding to the receptor was greatly reduced by the mutations D171A (TM4), D262A (TM6), and E288A/L290A (TM7), as reported previously (Table 4) (20, 37, 38). Of note, these mutations also affect SDF-1α binding and/or CXCR4 coreceptor activity (8). Unexpectedly, none of these three mutations affected the inhibition of MAb 12G5 binding by KRH-3955 (Table 4). Only the H281A (ECL3) mutant showed decreased inhibition of MAb 12G5 binding by KRH-3955 (Table 4). Interestingly, the same mutant modestly increased the blocking activity of AMD3100 against MAb 12G5 binding. In addition, the H281A mutation markedly impaired inhibition of MAb 12G5 binding by AMD3465, one of the prototype monocyclams (37). Further experiments with different CXCR4 mutants are necessary to identify the exact site(s) on CXCR4 targeted by this compound.

Pharmacological tests of KRH-3955 were performed with rats, and the compound was found to be bioavailable when administered orally (Table 5), which is favorable for anti-HIV drugs. However, the compound also indicated a long half-life after single-dose administration to rats, suggesting long-term accumulation of the compound in tissues, which can be either advantageous

in terms of inhibiting HIV-1 infection in hu-PBL–SCID mice (Table 6) or disadvantageous in terms of toxicity. Further studies are ongoing to determine the safety and pharmacokinetics of the compound in other animals such as dogs and monkeys. To evaluate the in vivo efficacy of KRH-3955, we used the hu-PBL–SCID mouse model and showed that oral administration of the compound strongly protected against X4 HIV-1 infection in this model system (Table 6). To achieve substantial replication of X4 HIV-1 in this system, recombinant IL-4 was added after human PBMC engraftment as described previously (23). Notably, KRH-3955 was administered only once 2 weeks before PBMC engraftment and was effective enough to block X4 HIV-1 infection, suggesting that the compound can be used as a preexposure prophylaxis agent to prevent HIV infection. This long-lasting antiviral effect of KRH-3955 can be partly explained by the strong affinity of the compound for CXCR4 (Fig. 6) and long-term accumulation of the compound in tissues.

In terms of safety of anti-HIV drugs, CCR5 antagonists are considered to be relatively safe because of the lack of obvious health problems in individuals homozygous for the CCR5 delta32 allele (27, 39). Indeed, maraviroc, a CCR5 antagonist, was approved by the U.S. FDA in 2007. In contrast, CXCR4 antagonists, which inhibit SDF-1α–CXCR4 interactions, may cause severe adverse effects because knocking out either the SDF-1α or the CXCR4 gene in mice causes marked defects such as abnormal hematopoiesis and cardiogenesis, in addition to vascularization of the gastrointestinal tract (32, 44, 52). However, no severe side effects have been reported for either AMD3100, a well-characterized CXCR4 antagonist, or AMD070, an oral CXCR4 antagonist, in human volunteers and/or HIV-infected patients. Milder side effects, including gastrointestinal symptoms and paresthesias, were common at higher doses of AMD3100. These results indicate the feasibility of using CXCR4 antagonists as anti-HIV-1 drugs in a clinical setting (21, 22, 41).

Besides the physiological roles mentioned above, the CXCR4–SDF-1 axis is also involved in various diseases such as cancer metastasis, leukemia cell progression, rheumatoid arthritis, and pulmonary fibrosis. CXCR4 antagonists such as AMD3100 and T140 have demonstrated activity in treating such CXCR4-mediated diseases (14, 46). In addition, AMD3100 is considered to be a stem cell mobilizer for transplantation in patients with cancers such as non-Hodgkin's lymphoma. Recently, AMD3100 has been shown to increase T-cell trafficking in the central nervous system, leading to significant improvement in the survival of West Nile virus encephalitis (29). Given its highly potent and selective inhibition of SDF-1–CXCR4 interaction and its bioavailability when administered orally, it is important to address whether KRH-3955 can also be used for such clinical applications.

One important issue to be addressed is whether HIV-1 strains resistant to other CXCR4 antagonists show cross-resistance to KRH-3955. In our preliminary studies, AMD3100-resistant HIV-1 (kindly provided by M. Baba, Kagoshima University) (4) showed ~19-fold resistance to KRH-3955 compared with parental NL4-3, whereas the resistant virus showed ~40-fold resistance to both AMD3100 and AMD070 in MT-4 cells (data not shown). Interestingly, the AMD3100-resistant HIV-1 strain was relatively sensitive to T22, another prototype CXCR4 antagonist. Thus, KRH-3955 target sites on CXCR4 seem to partially overlap those of AMD3100, although experiments with CXCR4 mutants do not support this idea. It is important to establish KRH-3955-resistant mutants and investigate whether they also show cross-resistance to other CXCR4 antagonists. Long-term culture experiments with PM1/CCR5 cells that express both CXCR4 and CCR5 infected with X4 HIV-1 in the presence of KRH-3955 are in progress.

In conclusion, KRH-3955 is a small-molecule antagonist of the CXCR4 receptor that is bioavailable when administered orally. The compound potently and selectively inhibits X4 HIV-1 infection both in vitro and in vivo. Thus, KRH-3955 is a promising antiviral agent for HIV-1 infection and should be evaluated for its clinical efficacy and safety in humans.

ACKNOWLEDGMENTS

We thank E. Freed for his critical review of the manuscript. We thank Y. Koyanagi, and R. Collman for generously providing plasmids and thank M. Baba for AMD3100-resistant HIV-1.

The following reagents were obtained from the NIH AIDS Research and Reference Reagent Program: saquinavir, subtype B HIV-1 primary isolates 92HT593, 92HT599 (N. Hasley), and 91US005 (B. Hahn) and AZT-resistant HIV-1 A018 (D. Richman). This work was supported in part by a grant for Research on HIV/AIDS from the Ministry of Health, Labor, and Welfare of Japan.

REFERENCES

1. **Adachi, A., H. E. Gendelman, S. Koenig, T. Folks, R. Willey, A. Rabson, and M. A. Martin.** 1986. Production of acquired immunodeficiency syndrome-associated retrovirus in human and nonhuman cells transfected with an infectious molecular clone. J. Virol. **59**:284–291.
2. **Alkhatib, G., C. Combadiere, C. C. Broder, Y. Feng, P. E. Kennedy, P. M. Murphy, and E. A. Berger.** 1996. CC CKR5: a RANTES, MIP-1α, MIP-1β receptor as a fusion cofactor for macrophage-tropic HIV-1. Science **272**:1955–1958.
3. **Amara, A., S. L. Gall, O. Schwartz, J. Salamero, M. Montes, P. Loetscher, M. Baggiolini, J. L. Virelizier, and F. Arenzana-Seisdedos.** 1997. HIV coreceptor downregulation as antiviral principle: SDF-1α-dependent internalization of the chemokine receptor CXCR4 contributes to inhibition of HIV replication. J. Exp. Med. **186**:139–146.
4. **Arakaki, R., H. Tamamura, M. Premanathan, K. Kanbara, S. Ramanan, K. Mochizuki, M. Baba, N. Fujii, and H. Nakashima.** 1999. T134, a small-molecule CXCR4 inhibitor, has no cross-drug resistance with AMD3100, a CXCR4 antagonist with a different structure. J. Virol. **73**:1719–1723.
5. **Baba, M., O. Nishimura, N. Kanzaki, M. Okamoto, H. Sawada, Y. Iizawa, M. Shiraishi, Y. Aramaki, K. Okonogi, Y. Ogawa, K. Meguro, and M. Fujino.** 1999. A small-molecule, nonpeptide CCR5 antagonist with highly potent and selective anti-HIV-1 activity. Proc. Natl. Acad. Sci. USA **96**:5698–5703.
6. **Baba, M., K. Takashima, H. Miyake, N. Kanzaki, K. Teshima, X. Wang, M. Shiraishi, and Y. Iizawa.** 2005. TAK-652 inhibits CCR5-mediated human immunodeficiency virus type 1 infection in vitro and has favorable pharmacokinetics in humans. Antimicrob. Agents Chemother. **49**:4584–4591.
7. **Bleul, C. C., M. Farzan, H. Choe, C. Parolin, I. Clark-Lewis, J. Sodroski, and T. A. Springer.** 1996. The lymphocyte chemoattractant SDF-1 is a ligand for LESTR/fusin and blocks HIV-1 entry. Nature **382**:829–833.
8. **Brelot, A., N. Heveker, M. Montes, and M. Alizon.** 2000. Identification of residues of CXCR4 critical for human immunodeficiency virus coreceptor and chemokine receptor activities. J. Biol. Chem. **275**:23736–23744.
9. **Coakley, E., C. J. Petropoulos, and J. M. Whitcomb.** 2005. Assessing chemokine co-receptor usage in HIV. Curr. Opin. Infect. Dis. **18**:9–15.
10. **Cocchi, F., A. L. DeVico, D. A. Garzino, S. K. Arya, R. C. Gallo, and P. Lusso.** 1995. Identification of RANTES, MIP-1α, and MIP-1β as the major HIV-suppressive factors produced by $CD8^+$ T cells. Science **270**:1811–1815.
11. **Collman, R., J. W. Balliet, S. A. Gregory, H. Friedman, D. L. Kolson, N. Nathanson, and A. Srinivasan.** 1992. An infectious molecular clone of an unusual macrophage-tropic and highly cytopathic strain of human immunodeficiency virus type 1. J. Virol. **66**:7517–7521.
12. **Connor, R. I., K. E. Sheridan, D. Ceradini, S. Choe, and N. R. Landau.** 1997. Change in coreceptor use correlates with disease progression in HIV-1-infected individuals. J. Exp. Med. **185**:621–628.
13. **Daar, E. S., K. L. Kesler, C. J. Petropoulos, W. Huang, M. Bates, A. E. Lail, E. P. Coakley, E. D. Gomperts, and S. M. Donfield.** 2007. Baseline HIV type 1 coreceptor tropism predicts disease progression. Clin. Infect. Dis. **45**:643–649.
14. **De Clercq, E.** 2005. Potential clinical applications of the CXCR4 antagonist bicyclam AMD3100. Mini Rev. Med. Chem. **5**:805–824.
15. **Deng, H., R. Liu, W. Ellmeier, S. Choe, D. Unutmaz, M. Burkhart, M. P. Di, S. Marmon, R. E. Sutton, C. M. Hill, C. B. Davis, S. C. Peiper, T. J. Schall, D. R. Littman, and N. R. Landau.** 1996. Identification of a major co-receptor for primary isolates of HIV-1. Nature **381**:661–666.

16. **Donzella, G. A., D. Schols, S. W. Lin, J. A. Este, K. A. Nagashima, P. J. Maddon, G. P. Allaway, T. P. Sakmar, G. Henson, E. De Clercq, and J. P. Moore.** 1998. AMD3100, a small molecule inhibitor of HIV-1 entry via the CXCR4 co-receptor. Nat. Med. **4**:72–77.
17. **Dorr, P., M. Westby, S. Dobbs, P. Griffin, B. Irvine, M. Macartney, J. Mori, G. Rickett, C. Smith-Burchnell, C. Napier, R. Webster, D. Armour, D. Price, B. Stammen, A. Wood, and M. Perros.** 2005. Maraviroc (UK-427,857), a potent, orally bioavailable, and selective small-molecule inhibitor of chemokine receptor CCR5 with broad-spectrum anti-human immunodeficiency virus type 1 activity. Antimicrob. Agents Chemother. **49**:4721–4732.
18. **Dragic, T., V. Litwin, G. P. Allaway, S. R. Martin, Y. Huang, K. A. Nagashima, C. Cayanan, P. J. Maddon, R. A. Koup, J. P. Moore, and W. A. Paxton.** 1996. HIV-1 entry into CD4$^+$ cells is mediated by the chemokine receptor CC-CKR-5. Nature **381**:667–673.
19. **Feng, Y., C. C. Broder, P. E. Kennedy, and E. A. Berger.** 1996. HIV-1 entry cofactor: functional cDNA cloning of a seven-transmembrane, G protein-coupled receptor. Science **272**:872–877.
20. **Gerlach, L. O., R. T. Skerlj, G. J. Bridger, and T. W. Schwartz.** 2001. Molecular interactions of cyclam and bicyclam non-peptide antagonists with the CXCR4 chemokine receptor. J. Biol. Chem. **276**:14153–14160.
21. **Hendrix, C. W., A. C. Collier, M. M. Lederman, D. Schols, R. B. Pollard, S. Brown, J. B. Jackson, R. W. Coombs, M. J. Glesby, C. W. Flexner, G. J. Bridger, K. Badel, R. T. MacFarland, G. W. Henson, and G. Calandra.** 2004. Safety, pharmacokinetics, and antiviral activity of AMD3100, a selective CXCR4 receptor inhibitor, in HIV-1 infection. J. Acquir. Immune Defic. Syndr. **37**:1253–1262.
22. **Hendrix, C. W., C. Flexner, R. T. MacFarland, C. Giandomenico, E. J. Fuchs, E. Redpath, G. Bridger, and G. W. Henson.** 2000. Pharmacokinetics and safety of AMD-3100, a novel antagonist of the CXCR-4 chemokine receptor, in human volunteers. Antimicrob. Agents Chemother. **44**:1667–1673.
23. **Ichiyama, K., S. Yokoyama-Kumakura, Y. Tanaka, R. Tanaka, K. Hirose, K. Bannai, T. Edamatsu, M. Yanaka, Y. Niitani, N. Miyano-Kurosaki, H. Takaku, Y. Koyanagi, and N. Yamamoto.** 2003. A duodenally absorbable CXC chemokine receptor 4 antagonist, KRH-1636, exhibits a potent and selective anti-HIV-1 activity. Proc. Natl. Acad. Sci. USA **100**:4185–4190.
24. **Kikukawa, R., Y. Koyanagi, S. Harada, N. Kobayashi, M. Hatanaka, and N. Yamamoto.** 1986. Differential susceptibility to the acquired immunodeficiency syndrome retrovirus in cloned cells of human leukemic T-cell line Molt-4. J. Virol. **57**:1159–1162.
25. **Koyanagi, Y., S. Miles, R. T. Mitsuyasu, J. E. Merrill, H. V. Vinters, and I. S. Chen.** 1987. Dual infection of the central nervous system by AIDS viruses with distinct cellular tropisms. Science **236**:819–822.
26. **Larder, B. A., G. Darby, and D. D. Richman.** 1989. HIV with reduced sensitivity to zidovudine (AZT) isolated during prolonged therapy. Science **243**:1731–1734.
27. **Liu, R., W. A. Paxton, S. Choe, D. Ceradini, S. R. Martin, R. Horuk, M. E. MacDonald, H. Stuhlmann, R. A. Koup, and N. R. Landau.** 1996. Homozygous defect in HIV-1 coreceptor accounts for resistance of some multiply-exposed individuals to HIV-1 infection. Cell **86**:367–377.
28. **Maeda, K., H. Nakata, Y. Koh, T. Miyakawa, H. Ogata, Y. Takaoka, S. Shibayama, K. Sagawa, D. Fukushima, J. Moravek, Y. Koyanagi, and H. Mitsuya.** 2004. Spirodiketopiperazine-based CCR5 inhibitor which preserves CC-chemokine/CCR5 interactions and exerts potent activity against R5 human immunodeficiency virus type 1 in vitro. J. Virol. **78**:8654–8662.
29. **McCandless, E. E., B. Zhang, M. S. Diamond, and R. S. Klein.** 2008. CXCR4 antagonism increases T cell trafficking in the central nervous system and improves survival from West Nile virus encephalitis. Proc. Natl. Acad. Sci. USA **105**:11270–11275.
30. **Murakami, T., T. Nakajima, Y. Koyanagi, K. Tachibana, N. Fujii, H. Tamamura, N. Yoshida, M. Waki, A. Matsumoto, O. Yoshie, T. Kishimoto, N. Yamamoto, and T. Nagasawa.** 1997. A small molecule CXCR4 inhibitor that blocks T cell line-tropic HIV-1 infection. J. Exp. Med. **186**:1389–1393.
31. **Murakami, T., T. Y. Zhang, Y. Koyanagi, Y. Tanaka, J. Kim, Y. Suzuki, S. Minoguchi, H. Tamamura, M. Waki, A. Matsumoto, N. Fujii, H. Shida, J. A. Hoxie, S. C. Peiper, and N. Yamamoto.** 1999. Inhibitory mechanism of the CXCR4 antagonist T22 against human immunodeficiency virus type 1 infection. J. Virol. **73**:7489–7496.
32. **Nagasawa, T., S. Hirota, K. Tachibana, N. Takakura, S. Nishikawa, Y. Kitamura, N. Yoshida, H. Kikutani, and T. Kishimoto.** 1996. Defects of B-cell lymphopoiesis and bone-marrow myelopoiesis in mice lacking the CXC chemokine PBSF/SDF-1. Nature **382**:635–638.
33. **Nakashima, H., M. Masuda, T. Murakami, Y. Koyanagi, A. Matsumoto, N. Fujii, and N. Yamamoto.** 1992. Anti-human immunodeficiency virus activity of a novel synthetic peptide, T22 ([Tyr-5,12, Lys-7]polyphemusin II): a possible inhibitor of virus-cell fusion. Antimicrob. Agents Chemother. **36**:1249–1255.
34. **Oberlin, E., A. Amara, F. Bachelerie, C. Bessia, J. L. Virelizier, F. Arenzana-Seisdedos, O. Schwartz, J. M. Heard, I. Clark-Lewis, D. F. Legler, M. Loetscher, M. Baggiolini, and B. Moser.** 1996. The CXC chemokine SDF-1 is the ligand for LESTR/fusin and prevents infection by T-cell-line-adapted HIV-1. Nature **382**:833–835.
35. **Richman, D. D., and S. A. Bozzette.** 1994. The impact of the syncytium-inducing phenotype of human immunodeficiency virus on disease progression. J. Infect. Dis. **169**:968–974.
36. **Roehm, N. W., G. H. Rodgers, S. M. Hatfield, and A. L. Glasebrook.** 1991. An improved colorimetric assay for cell proliferation and viability utilizing the tetrazolium salt XTT. J. Immunol. Methods **142**:257–265.
37. **Rosenkilde, M. M., L. O. Gerlach, S. Hatse, R. T. Skerlj, D. Schols, G. J. Bridger, and T. W. Schwartz.** 2007. Molecular mechanism of action of monocyclam versus bicyclam non-peptide antagonists in the CXCR4 chemokine receptor. J. Biol. Chem. **282**:27354–27365.
38. **Rosenkilde, M. M., L. O. Gerlach, J. S. Jakobsen, R. T. Skerlj, G. J. Bridger, and T. W. Schwartz.** 2004. Molecular mechanism of AMD3100 antagonism in the CXCR4 receptor: transfer of binding site to the CXCR3 receptor. J. Biol. Chem. **279**:3033–3041.
39. **Samson, M., F. Libert, B. J. Doranz, J. Rucker, C. Liesnard, C. M. Farber, S. Saragosti, C. Lapoumeroulie, J. Cognaux, C. Forceille, G. Muyldermans, C. Verhofstede, G. Burtonboy, M. Georges, T. Imai, S. Rana, Y. Yi, R. J. Smyth, R. G. Collman, R. W. Doms, G. Vassart, and M. Parmentier.** 1996. Resistance to HIV-1 infection in Caucasian individuals bearing mutant alleles of the CCR-5 chemokine receptor gene. Nature **382**:722–725.
40. **Schols, D., S. Struyf, J. Van Damme, J. A. Este, G. Henson, and E. De Clercq.** 1997. Inhibition of T-tropic HIV strains by selective antagonization of the chemokine receptor CXCR4. J. Exp. Med. **186**:1383–1388.
41. **Stone, N. D., S. B. Dunaway, C. Flexner, C. Tierney, G. B. Calandra, S. Becker, Y. J. Cao, I. P. Wiggins, J. Conley, R. T. MacFarland, J. G. Park, C. Lalama, S. Snyder, B. Kallungal, K. L. Klingman, and C. W. Hendrix.** 2007. Multiple-dose escalation study of the safety, pharmacokinetics, and biologic activity of oral AMD070, a selective CXCR4 receptor inhibitor, in human subjects. Antimicrob. Agents Chemother. **51**:2351–2358.
42. **Strizki, J. M., C. Tremblay, S. Xu, L. Wojcik, N. Wagner, W. Gonsiorek, R. W. Hipkin, C. C. Chou, C. Pugliese-Sivo, Y. Xiao, J. R. Tagat, K. Cox, T. Priestley, S. Sorota, W. Huang, M. Hirsch, G. R. Reyes, and B. M. Baroudy.** 2005. Discovery and characterization of vicriviroc (SCH 417690), a CCR5 antagonist with potent activity against human immunodeficiency virus type 1. Antimicrob. Agents Chemother. **49**:4911–4919.
43. **Strizki, J. M., S. Xu, N. E. Wagner, L. Wojcik, J. Liu, Y. Hou, M. Endres, A. Palani, S. Shapiro, J. W. Clader, W. J. Greenlee, J. R. Tagat, S. McCombie, K. Cox, A. B. Fawzi, C. C. Chou, C. Pugliese-Sivo, L. Davies, M. E. Moreno, D. D. Ho, A. Trkola, C. A. Stoddart, J. P. Moore, G. R. Reyes, and B. M. Baroudy.** 2001. SCH-C (SCH 351125), an orally bioavailable, small molecule antagonist of the chemokine receptor CCR5, is a potent inhibitor of HIV-1 infection in vitro and in vivo. Proc. Natl. Acad. Sci. USA **98**:12718–12723.
44. **Tachibana, K., S. Hirota, H. Iizasa, H. Yoshida, K. Kawabata, Y. Kataoka, Y. Kitamura, K. Matsushima, N. Yoshida, S. Nishikawa, T. Kishimoto, and T. Nagasawa.** 1998. The chemokine receptor CXCR4 is essential for vascularization of the gastrointestinal tract. Nature **393**:591–594.
45. **Takashima, K., H. Miyake, N. Kanzaki, Y. Tagawa, X. Wang, Y. Sugihara, Y. Iizawa, and M. Baba.** 2005. Highly potent inhibition of human immunodeficiency virus type 1 replication by TAK-220, an orally bioavailable small-molecule CCR5 antagonist. Antimicrob. Agents Chemother. **49**:3474–3482.
46. **Tamamura, H., H. Tsutsumi, H. Masuno, and N. Fujii.** 2007. Development of low molecular weight CXCR4 antagonists by exploratory structural tuning of cyclic tetra- and pentapeptide-scaffolds towards the treatment of HIV infection, cancer metastasis and rheumatoid arthritis. Curr. Med. Chem. **14**:93–102.
47. **Tanaka, R., A. Yoshida, T. Murakami, E. Baba, J. Lichtenfeld, T. Omori, T. Kimura, N. Tsurutani, N. Fujii, Z. X. Wang, S. C. Peiper, N. Yamamoto, and Y. Tanaka.** 2001. Unique monoclonal antibody recognizing the third extracellular loop of CXCR4 induces lymphocyte agglutination and enhances human immunodeficiency virus type 1-mediated syncytium formation and productive infection. J. Virol. **75**:11534–11543.
48. **Urano, E., T. Aoki, Y. Futahashi, T. Murakami, Y. Morikawa, N. Yamamoto, and J. Komano.** 2008. Substitution of the myristoylation signal of human immunodeficiency virus type 1 $Pr55^{Gag}$ with the phospholipase C-δ1 pleckstrin homology domain results in infectious pseudovirion production. J. Gen. Virol. **89**:3144–3149.
49. **Westby, M., M. Lewis, J. Whitcomb, M. Youle, A. L. Pozniak, I. T. James, T. M. Jenkins, M. Perros, and E. van der Ryst.** 2006. Emergence of CXCR4-using human immunodeficiency virus type 1 (HIV-1) variants in a minority of HIV-1-infected patients following treatment with the CCR5 antagonist maraviroc is from a pretreatment CXCR4-using virus reservoir. J. Virol. **80**:4909–4920.
50. **Xiao, L., D. L. Rudolph, S. M. Owen, T. J. Spira, and R. B. Lal.** 1998. Adaptation to promiscuous usage of CC and CXC-chemokine coreceptors in vivo correlates with HIV-1 disease progression. AIDS **12**:F137–F143.
51. **Yoshida, A., R. Tanaka, T. Murakami, Y. Takahashi, Y. Koyanagi, M. Nakamura, M. Ito, N. Yamamoto, and Y. Tanaka.** 2003. Induction of protective immune responses against R5 human immunodeficiency virus type 1 (HIV-1) infection in hu-PBL–SCID mice by intrasplenic immunization with HIV-1-pulsed dendritic cells: possible involvement of a novel factor of human CD4$^+$ T-cell origin. J. Virol. **77**:8719–8728.
52. **Zou, Y. R., A. H. Kottmann, M. Kuroda, I. Taniuchi, and D. R. Littman.** 1998. Function of the chemokine receptor CXCR4 in haematopoiesis and in cerebellar development. Nature **393**:595–599.

Int J Hematol (2010) 91:140–145
DOI 10.1007/s12185-009-0467-2

CASE REPORT

Successful unrelated bone marrow transplantation for a human immunodeficiency virus type-1-seropositive acute myelogenous leukemia patient following HAART

Yoko Oka · Haruko Tashiro · Mitsuho Mizutani-Noguchi · Ichiro Koga · Toshihiko Sugao · Ryosuke Shirasaki · Toshiyuki Miura · Nobu Akiyama · Kazuo Kawasugi · Shin Fujimori · Naoki Shirafuji

Received: 23 May 2009 / Revised: 10 November 2009 / Accepted: 2 December 2009 / Published online: 25 December 2009

Abstract The availability of highly active anti-retroviral therapy (HAART) has greatly improved the outcome of human immunodeficiency virus type-1 (HIV-1) infection and disease. We report here on a case of an HIV-1-seropositive patient with acute myelogenous leukemia who underwent a successful allogeneic unrelated bone marrow transplantation following HAART. A 40-year-old Japanese HIV-seropositive man underwent allogeneic unrelated bone marrow transplantation using a myeloablative pre-transplant-conditioning regimen. Neutrophil engraftment occurred on day +18, and donor chimerism was achieved on day +27. During pre- and post- transplantation, the HAART was not interrupted. Over 1 year after transplantation, the patient is alive and in continuous complete remission with undetectable levels of HIV-1 RNA. HAART can lead to a successful hematopoietic stem cell transplantation without severe opportunistic infections.

Keywords HIV-1 · AML · HAART · Unrelated bone marrow transplantation

Y. Oka · I. Koga · S. Fujimori
Department of Internal Medicine, Teikyo University School of Medicine, 2-11-1 Kaga, Itabashi-ku, Tokyo 173-8606, Japan

Y. Oka · H. Tashiro · M. Mizutani-Noguchi · T. Sugao · R. Shirasaki · N. Akiyama · K. Kawasugi · N. Shirafuji (✉)
Department of Hematology/Oncology, Teikyo University School of Medicine, 2-11-1 Kaga, Itabashi-ku, Tokyo 173-8606, Japan
e-mail: ramuji@med.teikyo-u.ac.jp

T. Miura
Department of Infectious Disease Control, International Research Center for Infectious Disease, The Institute of Medical Science, The University of Tokyo, 4-6-1 Shirokanedai, Minato-ku, Tokyo 108-8606, Japan

1 Introduction

Highly active anti-retroviral therapy (HAART) has greatly improved the outcome of human immunodeficiency virus type-1 (HIV-1) infection and disease [1]. Before the introduction of HAART, a high rate of unsuccessful autologous and allogeneic hematopoietic stem cell transplantation (HSCT) for HIV-1-seropositive patients was reported [2–5]. Thus, HIV-1-seropositive patients had been generally excluded from HSCT, even if they had hematological malignancies that would have been treated with HSCT in HIV-1-negative patients. However, successful autologous HSCT for hematological malignancies following HAART with a reduction in HIV-1 load and control of the CD4+ cell count has been reported, especially for HIV-1-associated lymphoma [6, 7]. On the other hand, allogeneic HSCT is an established therapy for some kinds of hematological disorders with curative potential; however, only a few cases of allogeneic HSCT for HIV-1-seropositive patients have been described since HAART became available [8–12].

HIV-1-seropositive patients have an increased risk of developing various kinds of malignancies, including non-Hodgkin's lymphoma and Kaposi's sarcoma [13, 14]. There are a few reports on the relationship between acute myeloid leukemia (AML) and HIV-1 infection. Sutton et al. [15] reported that the estimated risk of AML among HIV-1-infected adults was twice as that in the general population. We report here on an AML patient infected with HIV-1, who underwent unrelated bone marrow transplantation and is alive and well over one year after the transplant. To our knowledge, this is the first report on unrelated bone marrow transplantation for an AML patient with HIV-1.

2 Case report

In December 2006, a 39-year-old Japanese man was diagnosed with AML (FAB classification: M4). The white blood cell count of the patient was 131,000/μl. Bone marrow examination revealed that myelomonoblasts were expanded to 94%, which expressed CD13, CD33, CD34, and HLA-DR. Chromosomal analysis showed a normal karyotype. Screening for HIV-1 antibody by enzyme-linked immunosorbent assay (ELISA) was not performed at diagnosis. The patient underwent induction and consolidation chemotherapy in accordance with the JALSG AML 97 protocol [16] and achieved complete remission (CR). Because FLT3 internal tandem duplication of the bone marrow sample at the onset was positive, and it had continued to be detected, we planned an allogeneic bone marrow transplantation (BMT) during the first CR [17]. The patient had no HLA-identical sibling donor, so was registered for the Japan marrow donor program (JMDP) and underwent a screening test for HSCT. In October 2007, we found out that the patient was seropositive for HIV-1 by ELISA using his blood after obtaining informed consent. He described that he was a gay. We confirmed the presence of HIV-1 antibody by Western blot analysis, which detected bands against HIV-1 gp160, gp110/120, p68, p55, p52, gp 41, p34, and p24/25. At that time, the patient's HIV-1 load and CD4+ cell count were 2.9×10^4 copies/ml and 374/μl, respectively. The patient did not have any opportunistic infections. We started HAART consisting of emtricitabine (FTC) 200 mg, tenofovir (TDF) 300 mg, and efavirenz (EFV) 600 mg, which was determined with antiviral effects. The HIV-1 RNA load rapidly decreased to 61 copies/ml by December 2007. Retrospective analysis of the bone marrow sample showed that the patient had been infected with HIV-1 since he was diagnosed with AML (Fig. 1) [18, 19]; however, during standard chemotherapies before transplantation no severe infections were complicated.

In January 2008, an allogeneic BMT was performed during the first CR, using an unrelated HLA-matched male donor (Fig. 2). The number of transplanted nucleated cells was 3.1×10^8/kg. The patient was conditioned with a myeloablative regimen consisting of 12 Gy total body irradiation, 30 mg/kg intravenous etoposide, and 120 mg/kg intravenous cyclophosphamide. As prophylaxis for acute graft-versus-host disease (GVHD), administration of 3 mg/kg of cyclosporine A (CSP) was started on day −1, and short-term methotrexate was given on days +1, +3, +6, and +11. On HAART it was concerned that the patient could not take medication due to the pretransplant regimen-related toxicity. EFV shows a slow turnover (half time over 50 h); thus, in such a case only EFV was remaining in blood, which might lead to an induction of drug-refractory

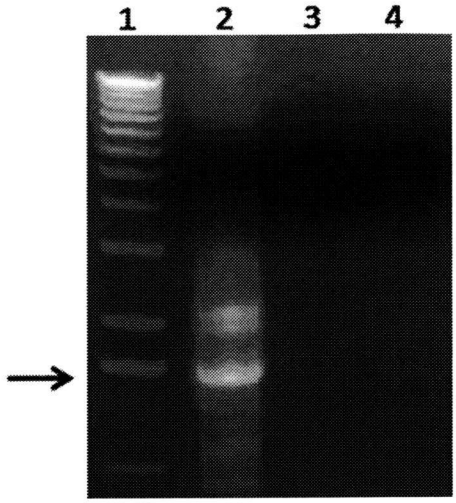

Fig. 1 Genomic PCR analysis. Total genomic DNA was isolated using Qiagen DNA blood mini kit (Qiagen Inc., Valencia, CA), and was subjected to PCR amplification. HIV-1 proviral gene sequence was amplified using nested PCR to generate *gag* products [18, 19]. Hot start was employed for the first and second PCR by incubating the reaction mixtures at 95°C for 2 min. Then, 35 cycles of amplification (94°C for 30 s, 60°C for 30 s, 72°C for 30 s) followed by a final incubation at 72°C for 2 min was applied for the first PCR. The second PCR involved the same conditions except for the amplification temperature (62°C). The primer pairs were: outer forward primer (5′-AAATCTCTA GCAGTGGCGCCCGAACAG-3′; positions 623–649 on HXB2); and reverse (5′-TAACCCTGCGGGATGTGGTATTCC-3′; positions 2849–2826); and inner forward primer (5′-GCGGCG ACTGGTGAGTA CGCC-3′, positions 734–754 on HXB2); and reverse (5′-TCCTTTAG TTGCCCCCCTATC-3′, positions 2314–2294 on HXB2). *Lane 1* MW marker, *Lane 2* bone marrow samples taken at diagnosis of the patient, *Lane 3* bone marrow samples at first CR and soon after the start of HAART (Dec. 2007), and *Lane 4* negative control. PCR products were analyzed by 2.5% TBE gel electrophoresis

HIV-1. We exchanged EFV for lopinavir (LPV) and ritonavir (RPV) referred to a half time.

Polymyxin-B sulfate was administered orally as prophylaxis for bacterial infection when the pretransplant conditioning started. 200 mg Fluconazole was given as prophylaxis against fungal infection. Acyclovir was used against herpes simplex virus infection until day +35. For the prophylaxis of *Pneumocystis Jiroveci*, trimethoprim-sulfamethoxazole was used. Cytomegalovirus (CMV) prophylaxis was started with 5000 mg of globulin every week from day −1. Ganciclovir as prophylaxis was not administered. Surveillance for CMV was performed by taking blood samples every week. The patient was received 5 μg/kg of granulocyte colony-stimulating factor (G-CSF) by continuous drip injection from day +1.

Febrile neutropenia developed requiring antibiotic therapy on day +6. Neutrophil, reticulocyte, and platelet engraftment was achieved on days +18, +18, and +22, respectively. Donor chimerism was achieved on day +27 in

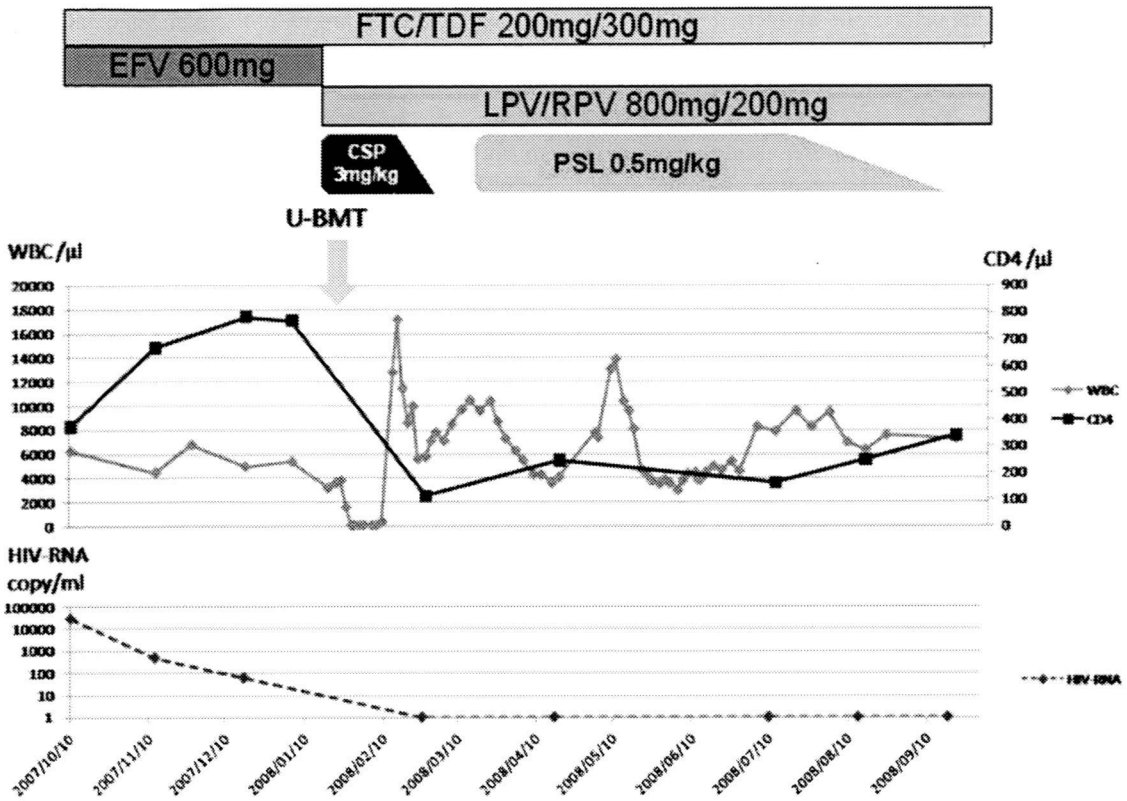

Fig. 2 Counts of HIV-1 viral load, CD4+ T-cells, and total white blood cells observed in the patient pre- and post-transplantation. *FTC* emtricitabine, *TDF* tenofovir, *EFV* efavirenz, *LPV* lopinavir, *RPV* ritonavir, *CSP* cyclosporine A, *PSL* predonisolone, *U-BMT* unrelated bone marrow transplantation

whole blood. Mild impairment of renal function developed (serum creatinine (Cr) level of 0.73 mg/dl on day 10, and 0.93 mg/dl on day 18). Owing to the rapid elevation of the serum level of CSP (971 ng/ml on day 10), which was probably due to interaction between CSP, LPV, RPV, and TDF, the administered dose of CSP was reduced. However, the patient's renal function worsened (Cr 1.14 mg/dl on day 20), and administration of CSP was stopped on day +21. Serum Cr level was 1.66 mg/dl on day 31, and the level was decreased thereafter. On day +53, CMV viremia developed without any evidence of CMV disease. We started intravenous administration of 10 mg/kg of ganciclovir, which promptly resolved the CMV viremia. On day +37, the patient developed acute skin GVHD (stage 2) and high fever without evidence of infection, and 0.5 mg/kg of predonisolone (PSL) was administered. After PSL treatment, the patient gradually recovered and was discharged on day +84.

Despite severe nausea, the patient could take all anti-HIV-1 drugs orally during pre- and post-transplantation. HIV-1 has not been detectable from day +31 until day +650. Although CD4+ cell count decreased to 114/μl on day +31, CD4+ cell count remained above 200/μl from day +202. Immunoglobulin level was sustained at the lower level (600–700 mg/dl after 6 months to 21 months after the transplantation). After 6 months from the transplantation, chronic extensive GVHD was observed, and PSL (1 mg/kg) with CSP was continued to be administered; however, no severe opportunistic infections were observed. At 21 months post-transplantation, the patient is alive and in continuous CR with undetectable levels of plasma HIV-1 RNA.

3 Discussion

In the HAART era, high-dose chemotherapy and autologous HSCT for HIV-1-seropositive patients can be successful [5–7]. Krishnan et al. [20] reviewed autologous transplantation for HIV-1-positive patients with lymphoma, and concluded that high-dose therapy with autologous stem cell rescue is feasible in HIV-1-infected patients with lymphoma following HAART. During chemotherapy, in combination with HAART, prompt reduction of HIV-1 load was reported [21, 22]. In our case, when HAART was introduced, prompt disappearance of HIV-1 was observed at PCR level (lane 3 of Fig. 1).

There are a few reports about allogeneic HSCT for HIV-1 carrier patients [8–12], and a brief summary is shown in Table 1. Recently, the Center for International Blood and Marrow Transplant Research (CIBMTR) reported allogeneic hematopoietic cell transplantation in human immunodeficiency virus-positive patients with hematological disorders [23]. Some problems are unresolved in allogeneic HSCT for HIV-1-seropositive patients treated with HAART, such as engraftment, GVHD prophylaxis and drug interaction, and opportunistic infection, in which the most important point is to check HIV-1 when a new patient suffering from a hematological malignancy is administered. In our case we fortunately found out his HIV-1 infection. CIBMTR reports that 31% of the HIV-1-infected patients with hematological malignancy who underwent HSCT were diagnosed before or at the onset of hematological malignancy. After this case we check HIV-1 antibody in all the new patients with hematological malignancies.

Among HIV-1-negative allogeneic BMT patients at our institute, the median time of myeloid, erythroid, and platelet engraftment is day +17.5, +21, and +23, respectively (unpublished). In this HIV-1-seropositive case, myeloid, erythroid, and platelet engraftments were similar to those of HIV-1-negative allogeneic BMT recipients. Tomonari et al. described a successful second unrelated cord blood transplantation for an HIV-1-seropositive patient using HAART, although the first cord blood transplantation showed prolonged bone marrow suppression and probable engraftment failure [10], in which HAART might have influenced the engraftment. Other reports describe similar engraftment periods for HIV-1-positive and negative patients who received allogeneic HSCT [8–12, 23, 24].

Previously, before the HAART era, some reports describing life-threatening opportunistic infections that often occur upon HSCT were published [2, 3]. Nowadays, HAART can lead to successful HSCT without severe opportunistic infections, control of the CD4+ cell count, and a decreased HIV-1 load. In our patient, cytomegalovirus reactivation was observed, which was promptly resolved by the administration of ganciclovir without CMV disease; other opportunistic infections did not occur. Sutton et al. [15] reported that a CD4+ cell count above 200/μl at the onset of AML was predictive of longer survival. Also, there are reported that before HAART era CD4 recovered very slowly after chemotherapy, and autologous and allogeneic transplantation [2–5, 23]. In HSCT, it seems likely that CD4+ cell count is as an important predictor of survival.

The optimum conditions for HAART before and during transplantation have not been established. Referred to the previous treatment-guidelines, no indication of HAART was determined to our case if he was not suffering from AML, because CD4+ cell count was above 350/μl; however, for the treatment of AML we used chemotherapy,

Table 1 Reported allogeneic HSCT cases for HIV-1-seropositive patients following HAART

	Diagnosis	Disease status	HAART	Transplant graft	Pretransplant conditioning	Engraftment	Outcome
Kang et al. [8]	t-AML	CR	I, S, L	Sibling PB	CY/Flu		Alive in CR: 2 years
Kang et al. [8]	HD	Primary refractory	Nf, ABC, L	Sibling PB	CY/Flu		Death: day +180 due to relapse
Sora et al. [9]	AML	CR	S, L, I→L, AZT, R	Sibling PB	BU/CY	Day +9	Alive in CR: 39 months
Tomonari et al. [10]	Ph ALL	CR	S, L, E	Unrelated CB	TBI/CY	Engraftment failure	To second CBT
Tomonari et al. [10]		Engraftment failure	(–)	Unrelated CB	Flu	Day +27	Alive in CR: 15 months
Wolf et al. [11]	AA		ABC, L, SQV, R → paused	Unrelated PB	CY/Flu	Day +18	Alive: 8 months
Woolfrey et al. [12]	AML	N/A	E, ABC, T	Unrelated PB	TBI/Flu		Death: day +301 due to GVHD/BO
Woolfrey et al. [12]	AML	N/A	E, ABC, L	Sibling PB	TBI/Flu		Alive: day +180
Our case	AML	CR	FTC/TDF, LPV/R	Unrelated BM	TBI/ETP/CY	Day +18	Alive in CR: 12 months

I inducates indinavir, *S* stavudine, *L* lamivudine, *Nf* nelfinavir, *ABC* abacavir, *AZT* zidovudine, *R* ritonavir, *E* efavirenz, *SQV* saquinavir, *T* tenofovir, *ALL* acute lymphocytic leukemia, *Ph* Philadelphia, *AA* aplastic anemia, *AML* acute myelogenous leukemia, *t-AML* treatment-related AML, *HD* Hodgkin's lymphoma, *CR* complete remission, *N/A* not described, *CB* umbilical cord blood, *PB* peripheral blood stem cell, *TBI* total body irradiation, *CY* cyclophosphamide, *Flu* fludarabine, *ETP* etoposide, *BU* busulfan, *GVHD* graft-versus-host disease, *BO* bronchiolitis obliterance